Department of Biomedical Sciences
International PhD School in Biomolecular and Biotechnological Sciences
Microbiology and Immunology

Director: Leonardo A. Sechi

Cycle XXVIII

Antiviral-Hyperactivation Limiting Therapeutics for the Treatment of Viral Diseases and Cancer

Supervisor:
Prof. Marco Pittau

PhD candidate:
Davide De Forni

Academic Year: 2014-2015

Table of Contents

1. ABSTRACT

Current anti-HIV drugs target several of viral enzymes that HIV requires to replicate and survive. Hyperactivation of the immune system is now recognized as the major driver of progression to AIDS and of the emergence of both AIDS-defining and non-AIDS events which negatively impact upon morbidity and mortality despite fully suppressive ART. AV-HALTs are a new class of antiretrovirals that both reduce HIV replication and excessive immune activation. By targeting a human rather than a viral enzyme the chances of the virus developing resistance are decreased, an improvement over traditional antiretroviral drugs. The proof of concept for this new class of drugs was achieved with a Phase IIa study in which the HU/ddI combination (first generation AV-HALTs) safely achieved the goals established for the AV-HALT class. The idea of AV-HALTs was further expanded in order to join both the antiproliferative and antiviral activities into a single molecule. CDK9 inhibitors were tested with the goal to identify second generation AV-HALTs. Compounds with good toxicity and activity profile were moved to preclinical development and were tested for ADME properties and preliminary *in vivo* experiments in rodent species. In addition, CDK9 inhibitors were found to be active against other viruses such as HSV-1, HSV-2, EBV and HPV. This class of compounds also proved to inhibit proliferation of tumor cells both *in vitro* and *in vivo*.

2. INTRODUCTION

2.1. HIV

Human Immunodeficiency Virus Type 1 (HIV-1) is a lentivirus of the family of the Retroviridae. The virus targets the host immune system ($CD4^+$ T cells and monocytes) and HIV-1 infection is characterized by a decline in T cell count and function, leading to a weakened immune system. HIV-1 virion's diploid genome consists of two single-stranded RNA molecules within a host-derived lipid bilayer. Infection of host cells by HIV-1 begins with the binding of the viral envelope glycoprotein (gp120) to specific receptors present at the plasma cell membrane. The main receptor for HIV-1 is the CD4 molecule which is expressed by T-helper lymphocytes, macrophages and dendritic cells. Binding of gp120 to CD4 molecule initiates the process of HIV-1 absorption to the target cell membrane followed by conformational changes in gp120 that enable it to bind to a co-receptor, the C-C chemokine receptor type 5 (CCR5) and the C-X-C chemokine receptor type 4 (CXCR4). Further conformational changes occur prompting to the exposure of the viral envelope glycoprotein gp41 ultimately leading to viral envelope fusion with target cell membrane.

Following entry of HIV-1 into the host cell, the viral core particle is released and the viral RNA is converted into double-stranded linear DNA by the viral reverse transcriptase. The core-DNA complex (or preintegration complex) is then imported into the nucleus of the host cell, nuclear entry is mediated by Vpr and Vif accessory proteins, as well as by nuclear localization signals. Viral integrase protein inserts the viral genome into the host cell chromosome in transcriptionallly active regions of the genome. Control of HIV-1 gene expression is regulated by both cellular and viral factors. The HIV-1 RNA genome contains 9 open reading frames and is about 9 kilobases in length. After integration, cellular factors mediate transcription of viral transcription factors located on the pol or env genes. Tat protein increases the transcription rate. After env gene has been transcribed Rev protein binds both spliced RNA (used for structural proteins) and unspliced RNA (used for genome

packaging) mediating export from the nucleus. Viral structural proteins are located on the gag gene and are transcribed and translated into a pre-protein (pr55) which is cleaved upon maturation of the virus. Another pre-protein is derived from gag-pol and yields the viral protease, integrase and reverse transcriptase (RT). Env gene is transcribed and translated into a gp160 pre-protein which travels to the cell membrane where, during virion formation, it is cleaved into gp120 and gp41. Other 3 regulatory proteins are obtained from env mRNA: Vpr (aids in the transport of cDNA into the nucleus), Vpu (aids in virion assembly) and Vif (important in maintaining infection efficiency). Figure 1 illustrates the HIV life cycle.

Figure 1. HIV life cycle (from UNAIDS website)

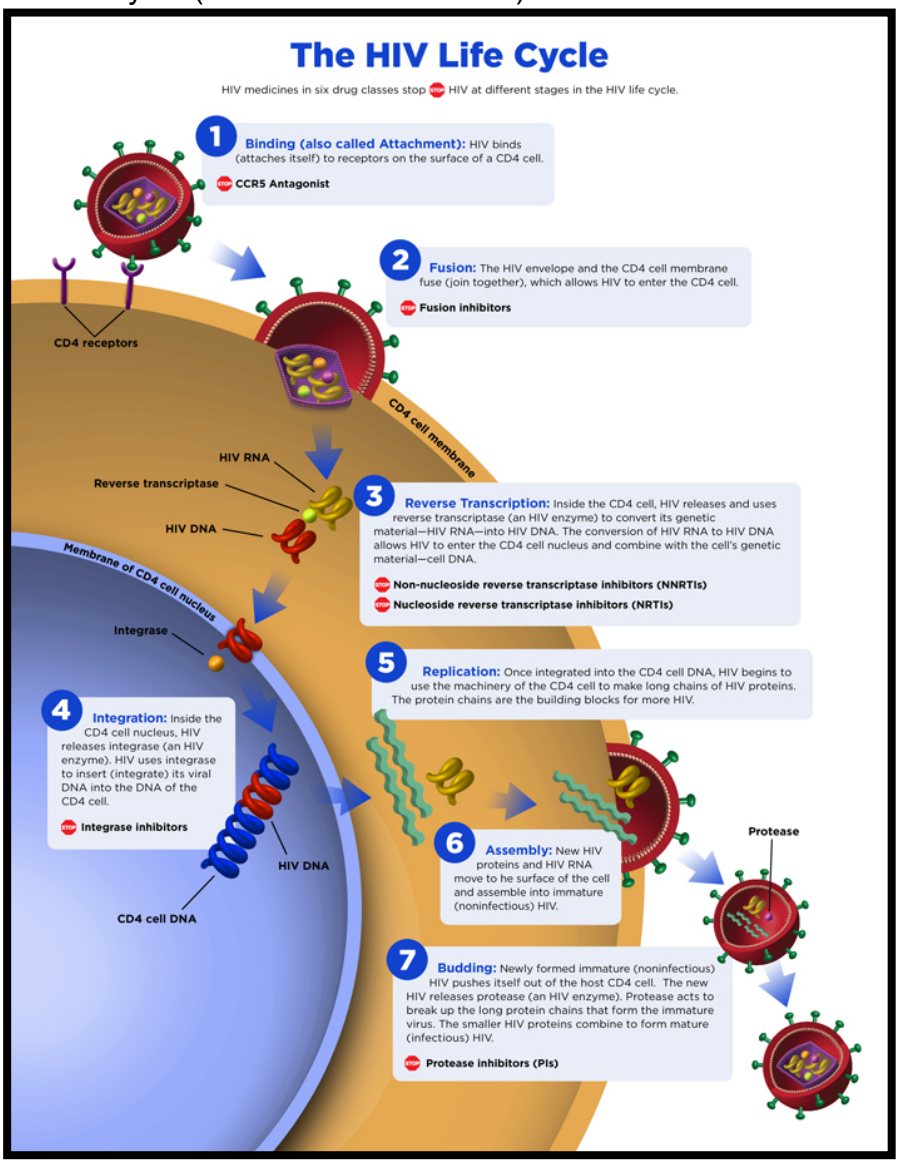

2.2. Transmission, natural course of HIV infection and epidemiology

HIV can be transmitted mainly by three routes: unprotected sexual intercourse, blood transfusion and from mother to child during pregnancy. In the absence of treatment, HIV infection leads to a progressive loss of circulating $CD4^+$ T lymphocytes which results in the immune dysfunction which is defined as AIDS (Acquired Immunodeficiency Syndrome).

Figure 2. Natural course of HIV infection (from UNAIDS website)

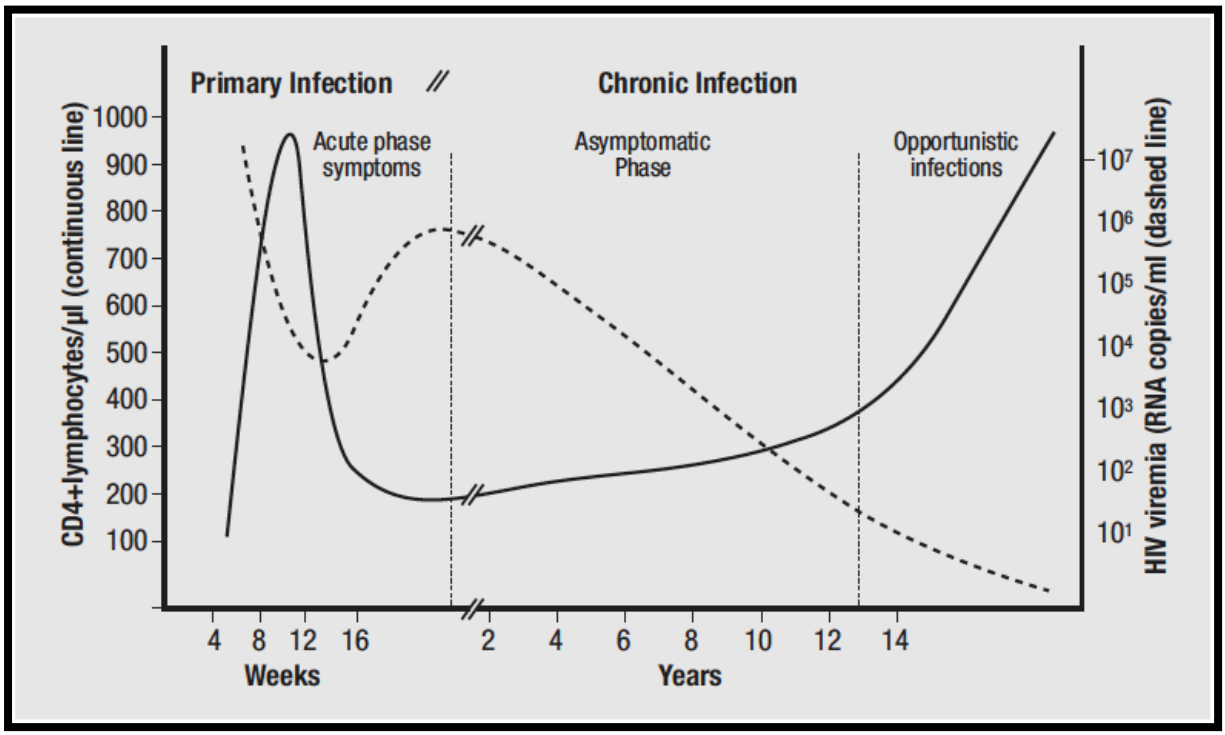

Since the beginning of the epidemic, almost 78 million people have been infected with the HIV virus and about 39 million people have died of HIV. Globally, 36.9 million [34.3–41.4 million] people were living with HIV at the end of 2014. An estimated 0.8% of adults aged 15–49 years worldwide are living with HIV, although the burden of the epidemic continues to vary considerably between countries and regions. The highest prevalence of HIV infection remains in Sub-Saharan Africa, there were 25.8 million people living with HIV in 2014 and there were 790,000 AIDS-related deaths (Table 1).

Table 1. Regional HIV data in 2014 (from UNAIDS website)

Region	People living with HIV 2014		New HIV infections 2014			AIDS-related deaths 2014 (total)
	total	children	total	adults	children	
Sub-Saharan Africa	**25.8 million** [24.0 million–28.7 million]	**2.3 million** [2.2 million–2.5 million]	**1.4 million** [1.2 million – 1.5 million]	**1.2 million** [1.1 million–1.3 million]	**190 000** [170 000-230 000]	**790 000** [670 000-990 000]
Asia and the Pacific	**5.0 million** 4.5 million-5.6 million	**200 000** [180 000–230 000]	**340 000** [240 000-480 000]	**320 000** [230 000–450 000]	**21 000** [16 000-27 000]	**240 000** [140 000-570 000]
Latin America	**1.7 million** [1.4 million-2.0 million]	**33 000** [29 000–40 000]	**87 000** [70 000-100 000]	**85 000** [68 000–100 000]	**2000** [1300-2900]	**41 000** [30 000-82 000]
Caribbean	**280 000** [210 000-340 000]	**13 000** [11 000–15 000]	**13 000** [9600-17 000]	**13 000** [9300–16 000]	**<500** [<500-<1000]	**8800** [5700-13 000]
Middle East and North Africa	**240 000** [150 000-320 000]	**13 000** [10 000–16 000]	**22 000** [13 000-33 000]	**20 000** [12 000–30 000]	**2400** [1800-3300]	**12 000** [5300-24 000]
Eastern Europe and Central Asia	**1.5 million** 1.3 million-1.8 million	**17 000** [14 000-19 000]	**140 000** [110 000-160 000]	**130 000** [110 000–160 000]	**1200** [<1000-1600]	**62 000** [34 000-140 000]
Western and Central Europe and North America	**2.4 million** [1.5 million-3.5 million]	**3300** [2200–4700]	**85 000** [48 000-130 000	**85 000** [47 000–130 000]	**<500** [<200-<500]	**26 000** [11 000-86 000]
GLOBAL	**36.9 million** [34.3 million-41.4 million]	**2.6 million** [2.4 million-2.8 million]	**2.0 million** [1.9 million-2.2 million]	**1.8 million** [1.7 million-2.0 million]	**220 000** [190 000-260 000]	**1.2 million** [980 000-1.6 million]

2.3. Therapy

Standard antiretroviral therapy (ART) consists of the combination of at least three antiretroviral (ARV) drugs to maximally suppress the HIV virus and stop the progression of HIV disease. Significant reductions have been seen in rates of death and suffering when use is made of a potent ARV regimen, particularly in early stages of the disease. There are six major types of drugs used to treat HIV/AIDS:

Entry Inhibitors interfere with the virus ability to bind to receptors on the outer surface of the cell it tries to enter. When receptor binding fails, HIV cannot infect the cell.

Fusion Inhibitors interfere with the virus ability to fuse with a cellular membrane, preventing HIV from entering a cell.

CCR5 antagonists block the CCR5 coreceptor on the surface of the immune cells preventing HIV from entering the cell.

RT Inhibitors prevent the HIV enzyme RT from converting single-stranded HIV RNA into double-stranded HIV DNA—a process called reverse transcription.

Integrase Inhibitors block the HIV enzyme integrase, which the virus uses to integrate its genetic material into the DNA of the cell it has infected.

Protease Inhibitors interfere with the HIV enzyme called protease, which normally cuts long chains of HIV proteins into smaller individual proteins. When protease does not work properly, new virus particles cannot be assembled.

To prevent strains of HIV from becoming resistant to a type of antiretroviral drug, healthcare providers recommend that people infected with HIV take a combination of antiretroviral drugs. Nonetheless, inherent limitations in current ART (most notably difficult adherence, short- and long-term toxicities, treatment-emergent resistance, and cost) continue to be associated with these multi-drug regimens.

In the course of chronic HIV infection a well-documented hyperactivation of the immune system occurs (Mahalingam 1993; Hunt 2003; Grossman 2006; Brenchley 2006), leading to a continuous cycle of increased T cell hyperproliferation and, ultimately, systemic inflammation. Chronic immune stimulation is due to persistent HIV-1 replication, microbial translocation and other factors, resulting in the eventual exhaustion of the immune system, accelerated senescence and, consequently, the onset of AIDS despite maximally suppressive ART regimens (Finkel 1995; Grossman 2000; McCune 2001; Hellerstein 2003).
Current anti-HIV therapy can significantly reduce viral replication and achieve ‘‘undetectable’’ levels of circulating HIV RNA (i.e., less than 50 copies/mL), however immune system hyperactivation, cellular hyperproliferation and inflammation do not

return to normal levels (Hunt 2003; Lesho 2006; Evans 1998).

This incomplete deactivation of the immune system is now considered the primary driver of a growing number of ‘‘non-AIDS defining events’’ including cardiovascular disease, liver disease, kidney disease, bone loss, increased rates of cancer, and accelerated aging even in individuals for whom today’s anti-HIV combinations have reduced the HIV virus to undetectable levels in their blood (Baker 2008; Ho 2010; Mitsuyasu 2008; Cauley 2007; Deeks 2003).

There is a growing recognition that successful long-term therapy for the treatment of HIV-1 infection should be disease modifying, not only reducing replicating virus but also directly diminishing the excessive chronic activation of the immune system (Hunt 2003; Brenchley 2006; Douek 2003; Silvestri 2005).

In order to address this unmet need, we developed an innovative core platform of antiviral-immune protective compounds called AntiViral-HyperActivation Limiting Therapeutics (AV-HALTs) designed to reduce both HIV-1 RNA levels and excessive chronic immune system hyperactivation. To accelerate drug development and establish the AV-HALT Proof of Concept in the treatment of HIV-1 in man, two available generic drugs, a direct-acting antiviral (didanosine, ddI) and a hyperactivation-limiting agent (hydroxyurea [HU]) were combined in a fixed-dose-combination (FDC) capsule known as VS411. This formulation was studied in a multinational Phase IIa trial in which it exhibited excellent safety and tolerability as well as providing solid proof-of-concept evidence for the AV-HALT paradigm by reducing HIV-1 RNA levels, increasing $CD4^+$ T cell counts and reducing the markers of immune system hyperactivation after only 28 days of therapy (Lori 2012).

VS411 is not being developed further due to concerns over the long-term toxicities associated with didanosine but successfully established the proof of concept that AV-HALTs can combine antiviral efficacy with rapid reductions in the immune system activation associated with HIV-1 disease. Work has been underway to screen, identify and develop single-molecule, second-generation AV-HALTs.

2.4. Targeting CDK9

Cyclin-dependent kinase 9 (CDK9) has been identified as a possible target for developing the new generation AV-HALTs.

CDK9 is a serine/threonine kinase that forms the catalytic core of the positive transcription elongation factor b (P-TEFb) (Loyer 2005; Yu 2011; Malumbres 2005; Romano 2008). This enzyme stimulates transcription elongation of most protein coding genes by RNA polymerase II (RNAPII) (Nechaev 2011). Activity of CDK9 is dependent on binding to a regulatory cyclin subunit (cyclin T1, T2a or T2b, K) and is further regulated through association with other macromolecules.

CDK9 has a typical protein kinase fold consisting of an N- and a C- terminal kinase lobe and a short C-terminal extension. The ATP-binding site is located between the N- and C-terminal lobes and contains highly conserved active site residues that coordinate ATP binding and phosphotransfer. Due to high sequence conservation among kinases and especially members of the CDK family, it is really challenging to generate selective CDK9 inhibitors (Krystof 2010; Wang 2008).

The majority of CDK9 is complexed with cyclin T1 in nuclear speckles and a small fraction of CDK9 is found in an apparently uncomplexed form in the cytoplasm. Studies have shown that nuclear P-TEFb exists in two functionally distinct complexes. Half of nuclear P-TEFb is found as an inactive complex associated with HEXIM1 (Hexamethylene Bis-Acetamide Inducible 1) and 7SK snRNA (Li 2005). Transcriptionally active P-TEFb associates with the bromodomain-containing protein 4 (Brd4) (Jang 2005).

2.5. CDK9 and HIV

During HIV-1 replication, the host RNAPII is recruited to the viral promoter within the long terminal repeat (LTR) and initiates transcription (Cujec 1997). RNAPII initiates transcription, but elongation of most of the transcripts is blocked by negative elongation factors (Fujinaga 2004; Ivanov 2000). The HIV-1 transcription transactivator Tat binds to the bulge of the HIV-1 RNA stem loop termed TAR (transactivation response element) that is found in all nascent HIV-1 messages and

recruits P-TEFb to the LTR (Price 2000; Zhou 2006). P-TEFb phosphorylates both the carboxyl-terminal domain (CTD) of RNAPII (Marshall 1996) and the negative elongation factors (Fujinaga 2004; Yamada 2006) allowing RNAPII to transition from abortive to productive elongation (Peterlin Mol Cell 2006).

2.6. CDK9 and other viruses

Significant amount of scientific evidence indicates that CDK9 is a key kinase involved in the life cycle not only of HIV but also of different viruses, including herpes viruses, flaviviruses and respiratory viruses. In the Herpes Simplex Virus type 1 (HSV-1) life cycle, it has been reported that CDK9 interacts with the immediate-early viral protein ICP22 and promotes Polymerase II. Inhibition of CDK9 through the CDK9 inhibitor DRB (5,6-dichlorobenzimidazone-1-β-D-ribofuranoside) or siRNA impedes viral transcription and causes a reduction in the expression of ICP22 (infected cell protein 22)-regulated mRNA and the late herpes proteins (Durand 2005; Ou 2013). In addition, roscovitine, an inhibitor of both CDK2 and CDK9, has been shown to attenuate Herpes Simplex Virus type 2 (HSV-2) replication (Schang 2002). Human Cytomegalovirus (HCMV) induces RNAPII CTD phosphorylation for immediate-early viral gene expression, coincident with increased CDK9 activity/localization (Tamrakar 2005). The HCMV encoded protein kinase, pUL69, has been shown to be strongly phosphorylated in HCMV-infected fibroblasts by CDKs. Analysis of CDK inhibitors in a pUL69-dependent nuclear mRNA export assay provided evidence for the functional impairment of pUL69 under conditions of suppression of CDK activity. Moreover, a direct impact of the complex CDK9/cyclin T1 has been demonstrated on the nuclear localization and activity of the viral regulator pUL69 (Rechter 2009, Feichtinger 2011). For Epstein-Barr Virus (EBV), it has been reported that the EBV encoded protein, EBNA 2 (Epstein-Barr nuclear antigen 2), phosphorylates RNAPII CTD in a CDK9 dependent manner, a dominant negative CDK9 can inhibit EBNA 2-activated transcription and the CDK9 inhibitor DRB can reduce the transcription rates of viral genes (Bark-Jones 2006). Moreover, EBNA 2 activates the viral promoter Cp through the CDK9/cyclin T1 complex to

produce all EBNAs required for EBV induced immortalization (Palermo 2011).
In a study it has been shown that recruitment of P-TEFb, which interacts with Brd4 in transcription activation, is important for transcription activation activity of E2. Furthermore, chromatin immunoprecipitation analyses demonstrate that P-TEFb is recruited to the actual papillomavirus episomes. Interaction of E2 with cellular chromatin through Brd4 correlates with its papillomavirus transcription activation function since JQ1(+), a bromodomain inhibitor that efficiently dissociates E2-Brd4 complexes from chromatin, potently reduces papillomavirus transcription (Helfer 2014).
In Dengue Virus (DENV), the DENV core protein and P-TEFb work in concert to enhance the IL-8 gene expression associated with DENV infection (Li 2010). In the Influenza virus life cycle, it has been reported that the CDK9/cyclin T1 complex serves as an adapter to mediate the interaction of vRNP (ribonucleoprotein) and RNAPII to promote viral transcription. Depletion of cyclin T1 by RNA interference has been shown to inhibit viral transcription and replication (Zhang 2010). In the case of Respiratory Syncytial Virus (RSV), CDK9 activity has been reported to be required for the RSV-inducible NF-kB-dependent gene expression (Brasier 2011).

2.7. CDK9 and cancer

To date, over 20 potent CDK inhibitors undergo phase I-II clinical trials in patients with different cancers (Lapenna 2009; Krystof 2010; Dickson 2009; Peyressatre 2015).
CDK9 inhibition leads to the downregulation of transcriptionally inducible genes with short half-lives, including cell cycle regulators and antiapoptotic factors (Lam 2001). Although the drugs target several CDKs, it has been proposed that the induction of apoptosis arises primarily due to the inhibition of CDK9 (Gojo 2002; MacCallum 2005; Santo 2010; Lam 2001). Inhibition of transcription through inhibition of CDK9 leads to a rapid decrease not only of D-type cyclins, that support uncontrolled proliferation, but also of antiapoptotic proteins XIAP (X-linked inhibitor of apoptosis protein) and Mcl-1 (Myeloid Cell Leukemia 1). Similarly, the induction of chronic

lymphocytic leukemia cells death induced by flavopiridol, SNS-032 or roscovitine is also mediated by the repression of transcription due to CDK9 inhibition and concomitant down-regulation of XIAP and Mcl-1 (Chen 2005; Chen 2009; Hahntow 2004). A dependence on the expression of antiapoptotic proteins is not exclusive to multiple myeloma or chronic lymphocytic leukemia. Experimental compound CR8, a congener of roscovitine, potently induces apoptosis in neuroblastoma cells, accompanied by Mcl-1 down-regulation both at the mRNA and protein levels (Bettayeb 2010). Similarly, compound VER-54505 reduced levels of Mcl-1 and XIAP in human osteosarcoma cell line U2OS (Scrace 2008). As a part of the positive transcriptional regulatory complex, CDK9 interacts also with the androgen receptor (AR) to enhance transcription activity (Lee 2001). CDK9 regulates the androgen receptor through S81 phosphorylation and this is an important step in regulating not only its transcriptional activity, but also for prostate cancer cell growth (Gordon 2010). It has been shown that pharmacological inhibition of CDK9 by flavopiridol resulted in decreased AR transcription.

3. MATERIALS AND METHODS

3.1. Compounds

A library of novel synthetic CDK9 inhibitors has been screened in order to identify safe compounds with dual antiproliferative and antiviral activity (second generation AV-HALTs).

3.2. *In vitro* CDK9/cyclin T assay

The activity of the compounds described in the present invention can be determined by measuring the phosphorylation of a fluorescently-labeled peptide by human CDK9/cyclin T kinase complex by fluorescent polarization using a commercially available IMAP (Immobilized Metal Ion Affinity-Based Fluorescence Polarization) Screening Express Assay Kit (Molecular devices).

Test compounds were diluted in 100% DMSO (dimethyl sulfoxide) to 5 mM stock concentration, then further dilutions were made in H_2O or 100% DMSO to desirable concentrations.

Each reaction consisted of 5 nM enzyme: CDK9/cyclin T (Proqinase cat# 0371-0345-1), 400 nM TAMRA-Rbtide (synthetic 15-mer peptide derived from human retinoblastoma tumor suppressor protein labelled with TAMRA dye, Genecust Europe), 12 µM ATP (=Km_{app}, Sigma-Aldrich) and kinase buffer: 20 mM MOPS pH 7 (Sigma-Aldrich), 1 mM DTT (Sigma-Aldrich), 10 mM $MgCl_2$ (Sigma-Aldrich), 0.01 % Tween 20 (Sigma-Aldrich).

For each reaction, 4 or 6 µL containing TAMRA-Rbtide, ATP and kinase assay buffer were combined with 2 µL diluted compound in H_2O or 0.028 µL compound in 100% DMSO. The kinase reaction was started by the addition of 2 µL diluted enzyme. The reaction was allowed to run for 1 hour at room temperature. The reaction was stopped by adding 15 µL IMAP beads (1:400 beads in progressive (100 % buffer A) 1X buffer). After an additional 1 hour, fluorescent polarization (Ex: 550-10 nm, Em: 590-10 nm, Dich: 561 nm) was measured using an Analyst GT (Molecular devices).

3.3. Drug toxicity analysis

Peripheral blood mononuclear cells (PBMC) were obtained from healthy donors by separation over Ficoll-Hypaque (GE Healthcare). After separation PBMC were washed in RPMI 1640 medium (BioWest) supplemented with 10% heat-inactivated fetal bovine serum (FBS, Gibco BRL), 2 mmol/L L-glutamine, 50 IU/mL penicillin, and 50 µg/mL streptomycin (all from BioWest), referred to as complete medium (CM), and the viable cells were counted by trypan blue (Gibco BRL) exclusion. PBMC were then suspended at 2 x 10^6 cell/mL in CM supplemented with 5 µg/mL of phytohemoagglutinin-P (PHA, Sigma Aldrich) in 75 cm^2 flasks (Sarstedt) and cultured for 2 days at 37°C in a humidified atmosphere supplemented with 5% CO_2. PBMC were then washed in CM, counted by trypan blue exclusion, suspended in CM supplemented with 20 IU/mL of interleukin-2 (IL-2, Boehringher-Mannerheim) and seeded in a 96-well plate (Costar Corning Incorporate) at 10^5 cells/well (200 µL CM per well). Cells were left untreated (NT) or treated with different concentrations of the compounds. After 7 days of incubation at 37°C cells were counted by trypan blue exclusion. Viability was expressed as the percentage of alive cells compared to the NT, indicated as 100%. Toxic dose 50% (TD_{50}, concentration inducing 50% cell death compared to NT) was calculated by interpolation of the dose-response curve.

3.4. Analysis of the effect of the compounds on cell proliferation and apoptosis

$CD4^+$ cells were separated by positive selection with anti-CD4 coated magnetic beads (Miltenyi Biotech Inc.) from peripheral blood mononuclear cells (PBMC) obtained from healthy, normal donors. Cells were stained with carboxyfluorescein succinimidyl ester (CFSE; Invitrogen) to trace cell divisions. Cells were suspended at a final concentration of 2.5 x 10^6 cells/mL in CM. $CD4^+$ cells were cultured for 5 days without stimulation then re-suspended in CM supplemented with 5 µg/mL PHA, after 2 additional days of culture, IL-2 at a concentration of 20 IU/mL was added, then cells were cultured for an additional 3 days. Cells were treated with compounds from day 1 to day 10. At day 10 proliferation was determined through CFSE flow

cytometric analysis. For data analysis, the mitotic index (M) was used, calculating the sum of mitotic events at each proliferation cycle. To extract a relative number, M was normalized to the total number of cells acquired using the equation $M = \sum(X_n(T) - X_n(T)/2n)$, that gives the number of mitotic events from the experimentally obtained values of the proportion of T cells under each division peak n (X_n) and the total T cells (T). To study the effect of the compounds on apoptosis $CD4^+$ cells were cultured as described above and at day 10 cells were stained with Annexin V and 7-AAD (7-aminoactinomycin D), in order to determine the percentage of early, late and total apoptotic events. When possible IC_{50} (concentration increasing of 50% total apoptotic effect compared to control) was calculated.

3.5. Study of the antiviral activity of the drugs on HIV-1 replication in resting/activated cells

$CD4^+$ cells were obtained as described above and then infected with HIV-1 NL 4.3 at a MOI (multiplicity of infection) of 0.001. Cells were cultured without stimulations for 5 days then stimulated with PHA/IL-2 as described before. Cells were treated with compounds from day 1 to day 10. The control was left untreated. After 10 days of incubation at 37°C supernatants were harvested and HIV-1 p24 Ag was measured by ELISA (Enzyme-Linked ImmunoSorbent Assay, Helvetica Health Care) in order to determine viral replication.

3.6. Mitochondrial toxicity

BxPC-3 cells were rinsed with phosphate buffered saline (PBS), and incubated with 0.55% trypsin and 0.2% EDTA (Biowest) for 5 min at 37°C. Fresh medium was then added and the viable cells were counted by trypan blue exclusion. BxPC-3 cells were plated in 6-well plates at a concentration of $2.5x10^5$ cells/well. Every 7 days of culture the cells were split, counted and replated at the same starting concentration. At day 14 cells were harvested and stained with the lipophilic cationic probe JC-1 (5,5′,6,6′-tetrachloro-1,1′,3,3′-tetraethylbenzimidazolylcarbocyanine iodide, Molecular

Probes) and analyzed by flow cytometry to evaluate mitochondrial functionality.

3.7. ADME *(*absorption, distribution, metabolism, and excretion) studies

3.7.1. Thermodynamic solubility

Thermodynamic solubility of compounds was determined in phosphate buffer pH 7.4, at room temperature by the shake flask method. Quantification of the samples was performed on calibration curves prepared by dilution in acetonitrile (ACN) of a 2 mg/mL stock solution in DMSO.

A calibration curve (10 points) has been prepared from the working standard solutions by the appropriate dilution with ACN. Saturated solutions of the compounds were prepared by incubating about 2 mg in 1 mL of buffer for 24h at room temperature (25°C) under agitation. At the end of the incubation samples were filtered, aliquots (3) were diluted in ACN 1:100 and each sample was then injected three times into LC-MS/MS (liquid chromatography and mass spectrometry). Samples of the calibration curve were analysed on Shimazu UFLC with API 4500 Detector, Triple Quadrupole LC-MS/MS Mass spectrometer.

3.7.2. *In vitro* absorption in Caco-2

Caco-2 (colorectal adenocarcinoma, ATCC) monolayers were cultured on cell culture inserts. The transport from the apical to the basolateral side (A→B) across the Caco-2 monolayer was determined by adding the test compound to the apical side. In the (B→A) experiment, the test compound is added in the basolateral side and collected in the apical side.

After 2 hours of incubation, the basolateral side solution, together with the apical and the starting solutions, was analysed and quantified by LC-MS/MS. To maintain physiologically relevant conditions, the pH of the apical side was 6.5, while the pH of the basolateral side was 7.4. The apparent permeability (P_{app}) was calculated according to the following equation:

P_{app} = J/Co

where:

J=flux (dX/dt x A) and Co=donor concentration (μM) at t=0; dX/dt=change in mass (X, nmol) per time (t, sec), A=filter surface area (cm^2).

The apparent permeability of the test compounds, and their rank order, is always compared with two known reference compounds tested in the same experiment. Suggested absorption classification values are:

P_{app} > 50 nm/s: high;

P_{app} 10-50 nm/s: medium;

P_{app} < 10 nm/s: low.

3.7.3. Metabolic stability

The metabolic stability of the test compound was assayed in microsomes (for phase I metabolism). The test compound was pre-incubated for 10 minutes at 37°C in the appropriate buffer at pH 7.4 with microsomes (human and rat). After the pre-incubation period, the reaction was started (time 0) by adding the cofactors mixture; samples were taken at 30 minutes and added to acetonitrile containing an internal standard to stop the reaction. Samples were then centrifuged and supernatant analysed by LC-MS/MS. A control sample without cofactors was always added in order to check the chemical stability of test compound in the matrix. The rate constant k (min^{-1}), derived for the exponential decay equation, is used to calculate the rate of intrinsic clearance (Cli) of the compound using the following equation:

Cli (μL × min^{-1}× mg $protein^{-1}$) = k x V

where: V (μL × mg $protein^{-1}$) = incubation volume/mg protein added.

3.7.4. Inhibition of cytochrome P450

Inhibition of the most important cytochrome P450 isoforms (CYP1A2, CYP2C9, CYP2C19, CYP2D6, CYP3A4) was measured in specific assays, using specific substrates that become fluorescent upon CYP metabolism. Human recombinant P450 isoforms (Supersomes, Gentest) were employed together with the following

substrates: CEC (3-cyano-7-ethoxycoumarin) for CYP1A2 and CYP2C19; MFC (7-methoxy-4-(trifluoromethyl)-coumarin) for CYP2C9; AMMC (3-[2-(N,N-diethyl-N-methylammonium)ethyl]-7-methoxy-4-methylcoumarin) for CYP2D6; BFC (7-benzyloxy-4-(trifluoromethyl)-coumarin) for CYP3A4.

Control inhibitors were added in every experiment. Compound solutions were tested at single concentration (10 μM). The reaction was started by adding specific isoenzymes and substrates at 37°C. After the incubation period (15-45 minutes depending on the CYP isoform), the reaction was stopped and plates were read on a fluorimeter at the appropriate emission/excitation wavelengths. The percentage inhibition of control enzyme activity (without inhibitor) was calculated.

3.8. Preliminary toxicology study

The toxic profile of one compound was analyzed after single oral treatment at 500 mg/kg (suspension formulation) and after 5-day repeated oral treatment at 100 mg/kg (solution formulation) in CD1 mice. Satellite groups were also treated in parallel in order to evaluate the plasma exposure (pharmacokinetics, PK) after the administration of 500 mg/kg in suspension and prior and after the fifth day of treatment at 100 mg/kg. Formulations employed consisted of compound dissolved in 5% DMSO (Sigma-Aldrich) and 95% of a solution of 20% Soluplus (Sigma-Aldrich)/ 80% buffer pH 2 (w/w). All animals were weighed before treatment on the day of treatment and every following day till day 7. Clinical signs and mortality were monitored and reported at regular intervals.

Animals of PK group treated with 5x100 mg/kg were sampled from the mandibular plexus before the last treatment at day 5 (t=0) and at 0.5, 1, 2, 4, 8, 24 and 48 hr after the last treatment. Animals of PK group treated with 500 mg/kg were sampled from the mandibular plexus at 0.5, 1, 2, 4, 8, 24 and 48 hr.

Samples were analyzed on UFLC (Ultra Fast Liquid Chromatography) Shimazu AC20 coupled with a API 4500 Triple Quadrupole ABSciex.

3.9. PK study

Oral bioavailability and pharmacokinetic parameters were determined in the male rat. DMSO was added to the pre-weighted compound and vortexed 1 min. Solutol (after being heated at 50°C) was added to the compound and solution vortexed for 1 min. PBS was added slowly under agitation.

Formulations used in the study are summarized below.

Intravenous (IV) treatment: 3 mg/kg	7.98 mg 5% DMSO (665 µL), 5% Solutol (665 µL) in PBS pH 7.4 (11.97 mL) Administration volume: 5 mL/kg
Oral (per os, PO) treatment: 10 mg/kg	22 mg 5% DMSO (550 µL), 5% Solutol (550 µL) in PBS pH 7.4 (9.9 mL). Administration volume: 5 mL/kg

After IV treatment, blood was sampled from caudal vein at the following timepoints: 3, 10, 30, 60, 120, 240, 480, 1440 minutes.
After PO treatment (Oral gavage), blood was sampled from caudal vein at the following timepoints: 10, 30, 60, 120, 240, 360, 480 1440 minutes. Samples were analyzed on UFLC Shimazu AC20 coupled with a API 4500 Triple Quadrupole ABSciex.

3.10. HSV assay

Human foreskin fibroblast (HFF) cells were cultured in minimum essential media (MEM) with Earle's salts supplemented with 10% fetal bovine serum (FBS) and standard concentrations of penicillin and gentamicin (Prichard 2008).
A primary cytopathic effect (CPE) reduction assay was performed. Low passage (3-10) HFF cells were trypsinized, counted, and seeded into 96 well tissue culture plates in 0.1 mL of MEM supplemented with 10% FBS. The cells were then incubated for 24 h at 37^{o}C. The media was then removed and 100 µL of MEM

containing 2% FBS was added to all but the first row. In the first row, 125 µL of media containing the experimental drug was added in triplicate wells. Media alone was added to both cell and virus control wells. The drug in the first row of wells was then diluted serially 1:5 throughout the remaining. The plates were then incubated for 60 min and 100 µL of a virus suspension was added to each well, excluding cell control wells which received 100 µL of MEM. The plates were then incubated at 37^{o}C in a CO_2 incubator for three days. After the incubation period, media was aspirated and the cells stained with crystal violet in formalin for 4h. The stain was then removed and the plates were rinsed until all excess stain was removed. The plates were allowed to dry for 24 h and the amount of CPE in each row determined using a multiplate autoreader. EC_{50} (effective concentration 50%) and CC_{50} (cytotoxic concentration 50%) values were determined by comparing drug treated and untreated cells using a computer program.

3.11. EBV assay

A primary DNA hybridization assay was performed (Prichard 2007). Assays for EBV were performed in Akata cells that were induced to undergo a lytic infection. Cells were maintained in RPMI 1640 supplemented with 10% FBS, L-glutamine, penicillin and gentamicin at 37°C in a humidified 5% CO_2 atmosphere. Cells were passaged 2-3 days prior to performing the assay. Experimental compounds were diluted in 96-well plates to yield concentrations ranging from 20 to 0.0064 µM. Latently infected Akata cells were added to the plates to a final concentration of $4x10^5$ cells/mL, induced to undergo a lytic infection and incubated for 72 h.

An alkaline denaturation buffer (1.2 M NaOH, 4.5 M NaCl) was added to each well to denature the DNA and a 50 µL aliquot was aspirated through a nylon membrane. The membranes were then allowed to dry before equilibration in DIG Easy Hyb (Roche Diagnostics, Indianapolis, IN) at 56°C for 30 min. Specific digoxigenin (DIG)-labeled probes were prepared for each virus and corresponded to coordinates 96802–97234 in EBV genome. Membranes with EBV DNA were hybridized overnight and followed by sequential washes 0.2X SSC (Sodium Chloride Sodium Citrate) with

0.1% SDS (Sodium Dodecyl Sulphate) and 0.1X SSC with 0.1% SDS at the same temperature. Detection of specifically bound DIG probe was performed with anti-DIG antibody using the manufacturer's protocol (Roche Diagnostics). An image of the photographic film was captured and quantified with QuantityOne software (Bio-Rad) and compound concentrations sufficient to reduce the accumulation of viral DNA by 50% (EC_{50}), were interpolated from the experimental data. Cell viability was assessed with the CellTiter-Glo Luminescent Cell Viability Assay (Promega). Briefly, assay plates were incubated at ambient temperature for 30 min then 50 µL of CellTiter-Glo reagent was added to each well and the plates were mixed for 2 min on an orbital shaker to lyse the cells. Plates were then incubated for an additional 10 min at ambient temperature and the luminescence was quantified on a luminometer. CC_{50} (cytotoxic concentration 50%) was calculated.

3.12. HPV assay

A transient replication of HPV origin-containing plasmid in transfected HEK293 (human embryonic kidney) cells was performed. In this assay, vectors for expression of an HPV genotype-matched set of viral E1 and E2 proteins along with an HPV ori-containing plasmid were cotransfected into HEK293 cells. Cells were cultured in the absence or presence of the test compounds at 1, 10, and 100 µM. Low molecular weight DNA was harvested 2 days post-transfection and digested with Dpn1 and exonuclease III to remove unreplicated transfected plasmid DNA. The replicated DNA was then subjected to real time qPCR (quantitative polymerase chain reaction) analyses in triplicate. Two controls were performed. One was to omit the E1 expression vector to provide a background amount of undigested and unreplicated DNA. The other, positive control was treatment with the known inhibitor cidofovir. A toxicity assay based upon cell viability at the time of harvest on day 2 was performed alongside each transient replication assay in HEK293 cells. Compounds were added 4 hours post transfection at 1, 10, or 100 µM for a total exposure of 44 hr. Cell viability was evaluated through trypan blue staining. EC_{50} (effective concentration 50%) and CC_{50} (cytotoxic concentration 50%) values were determined.

3.13. MTS assay in cancer cell lines

The antiproliferative effect of the compounds was investigated *in vitro* in the following cell lines:

Jurkat: T cell leukemia cell line

HEC1A: endometrial carcinoma cell line

A2780: ovarian carcinoma cell line

MNK-45: gastric carcinoma cell line

H1229: lung cancer cell line

The cell lines were routinely maintained in RPMI supplemented with 1% glutamine (Biowest) and 10% fetal bovine serum (Gibco). The cytotoxic activity of the selected compounds was tested in the 5 cell lines using standardized MTS [(3-(4,5-dimethylthiazol-2-yl)-5-(3-carboxymethoxyphenyl)-2-(4-sulfophenyl)-2H-tetrazolium)] cytotoxic assays. Briefly, exponentially growing cells were seeded into 96-well plates at their optimal density in complete medium. 48-72 hours later cells were treated or not with seven different final concentrations (10, 5, 1, 0.5, 0.1, 0.05, 0.01 μM) of the selected compounds for 72 hours using six replicates each concentration. Drug dilutions were be performed in medium. Drug treatment lasted 72 hours at the end of which cell viability was assessed by MTS Colorimetric Assay (Promega). The experiment was repeated twice for each cell line. The Inhibitory Concentration 50% (IC_{50}) values were obtained by interpolating the generated dose-response.

3.14. Mouse Xenograft Model

Experiment was performed in collaboration with Mario Negri Institute of Pharmacological Research (Milan). The test compound was dissolved in N-methyl pyrrolidone (NMP) 5% (v/v), Polyethylene glycol 400 (PEG400) 85% (v/v) and Water 10% (v/v) to give a final 5 mg/mL solution. H1299 cell line was maintained in RPMI 1640 medium (Biowest), supplemented with 10% Foetal Bovine Serum (Gibco) and 1% glutamine (Biowest).

The experiment was performed using six-week old athymic female mice, provided by Harlan Italy Srl. Mice were maintained in the animal house under controlled

conditions (constant and controlled temperature and humidity) that allows to keep the Specific Pathogen Free status. Feeding regimen was *ad libitum*. To obtain tumor xenografts, 200 µL of cell suspension containing $7x10^6$ H1299 cells were sub-cutaneously injected into the flanks of each mouse. The growing tumor masses were measured through a Vernier caliper, and the tumor weights (1 mm^3 = 1 mg) were calculated by the formula: length x $(width)^2/2$. When tumor load reached about 120 mg, mice were randomized into the experimental groups, with body weight and tumor mass distributions balanced between the two groups. Mice were randomized in the following study groups:

- Vehicle (9 animals)
- Test compound 50 mg/kg/day (10 animals)

Compound and vehicle were orally administered at a dose volume of 10 mL/kg daily for 15 consecutive days (until day 35 post tumor implant).

Tumor size and mouse body weight were recorded three times a week from treatment start until the end of the study. Drug efficacy was calculated as T/C%, where T and C are the mean tumor weights of treated and control groups, respectively. Tolerability was evaluated on the basis of body weight loss (BWL) and clinical observation.

4. RESULTS

4.1. Screening of CDK9 inhibitors

A library of potential CDK9 inhibitors was screened in biochemical assay for CDK9 activity and selected hits (IC_{50} values < 1 μM) were tested in biological assay to determine AV-HALT characteristics.

Chemical structure of these compounds can not yet be revealed because compounds deriving from this library are still under active development by the company ViroStatics and covered by confidentiality measures.

A panel of tests has been optimized in order to characterise compounds including measures of toxicity (viability, apoptotic effect, mitochondrial toxicity) and measures of activity (inhibition of cell proliferation, inhibition of HIV replication). The goal was to find compounds with a good toxicity profile and inhibiting both proliferation of the cells and viral replication within a single chemical entity (i.e. AV-HALT compounds).

VS411 is the comparator prototype AV-HALT and was employed in all experiments as a reference being already tested in clinical studies. A concentration of 100 μM hydroxyurea and 2 μM didanosine (corresponding to the *in vivo* peak plasma concentrations after administration of 600 mg hydroxyurea and 400 mg didanosine, a dose combination that proved to be both active and safe in clinical trial) was chosen to be tested *in vitro* as a reference to determine ranges of toxicity and activity for the screening of the compounds.

4.2. Determination of cytotoxicity in peripheral blood mononuclear cells

PHA/IL-2 stimulated peripheral blood mononuclear cells were exposed to different concentrations of the compounds for 7 days. Then viability was determined through Trypan blue staining and expressed as percentage of untreated control (control=100% viability). A dose response curve was built for each of the compounds in order to determine the TD_{50} by interpolation of the data. An example of a dosage-response relationship is shown in Figure 3 for one representative compound.

Figure 3. Determination of TD_{50} for compound VS1

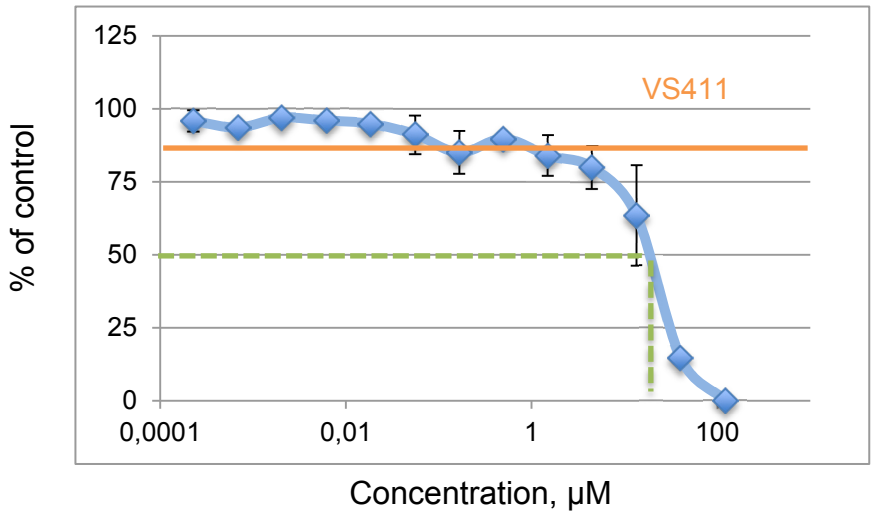

Viability of VS411 (100 μM HU/2 μM ddI) is indicated by the red line (80% viability compared to untreated control) while dotted line shows how TD_{50} is interpolated.

4.3. Determination of apoptotic effect in CD4+ T cells

$CD4^+$ T cells derived from peripheral blood mononuclear cells by magnetic bead positive separation were exposed to different concentrations of the drugs for 10 days. Apoptotic events were then detected through Annexin V/7-AAD staining and cytofluorimetric analysis allowing determination of both early (Annexin V+/7-AAD-) and late (Annexin V+/7-AAD+) apoptotic events. Percentage of apopotic cells was compared to control and VS411 in order to identify and exclude those compounds being more proapototic than VS411 and in general inducing more than 30% total apoptotic events compared to untreated control.

A picture of the apoptotic events induced by compound VS1 is shown in Figure 4 in comparison with VS411.

Figure 4. Determination of apoptotic effect of the compounds

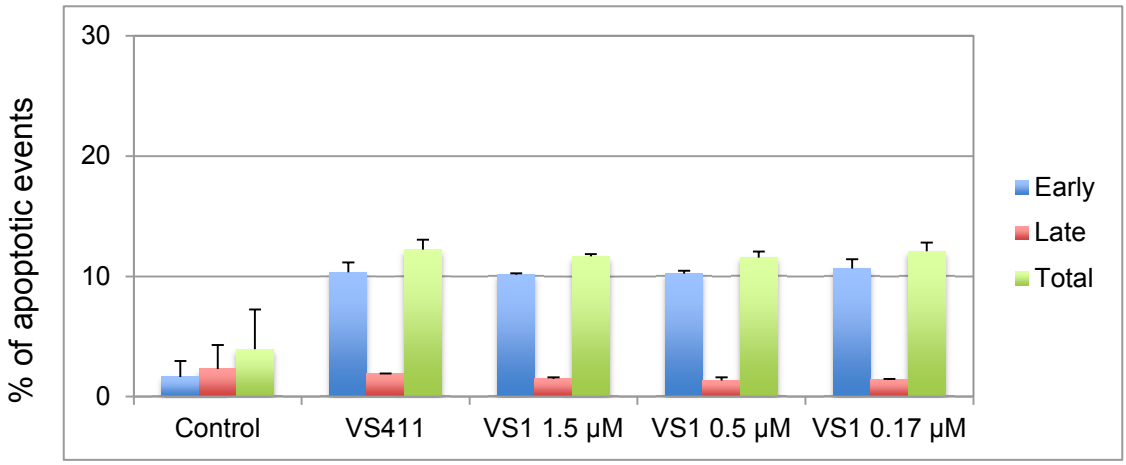

Both compound VS1 and VS411 did not induce significant apoptotic effect compared to untreated control. There were no relevant differences between early and late apoptotic events at the tested doses.

4.4. Determination of mitochondrial toxicity

The human pancreatic cell line BxPC3 was exposed to different concentrations of the compounds, after 14 days on treatment cells were stained with JC-1 and analyzed by flow cytometry. MTI was calculated and compared to that of VS411 in order to exclude compounds inducing a damage to mitochondrial membrane.

Target MTI was < 40% compared to maximal toxicity induced by the reference compound Valinomycin.

Figure 5. Determination of mitochondrial toxicity of the compound VS1

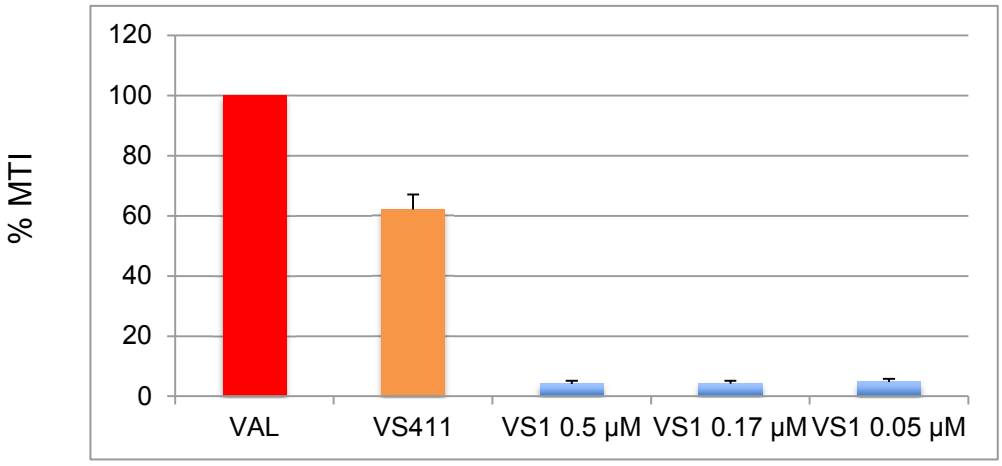

VS411 induces mitochondrial toxicity (MTI=61), in fact didanosine (the antiviral component of this drug combination) is known to cause this effect *in vitro* and increases risk of pancreatitis and hepatitis *in vivo* (Benbrik J Neurol Sci 1997; Bissuel J Intern Med 1994; Brinkman AIDS 1998). VS1 did not induce mitochondrial toxicity at the tested concentrations (at concentrations inhibiting both cellular proliferation and HIV replication).

4.5. Determination of antiproliferative effect in CD4+ T cells

In a 10 days experiment cells were stained with the tracer CFSE on Day 1 of the experiment and analyzed by flow cytometry in order to determine the number of mitotic events and the mitotic index. Antiproliferative activity (AP) was calculated as the inhibition of cell proliferation = 100 minus the % mitotic index compared to the control (AP of control = 0%). AP_{50} was calculated by interpolation of the dose response curve as shown in Figure 6. Target was not to completely suppress cell proliferation in order to avoid immune suppression *in vivo*.

VS411 antiproliferative activity is shown by the orange line (80% inhibition of cell proliferation compared to control).

Figure 6. Determination of antiproliferative activity of the compound VS1

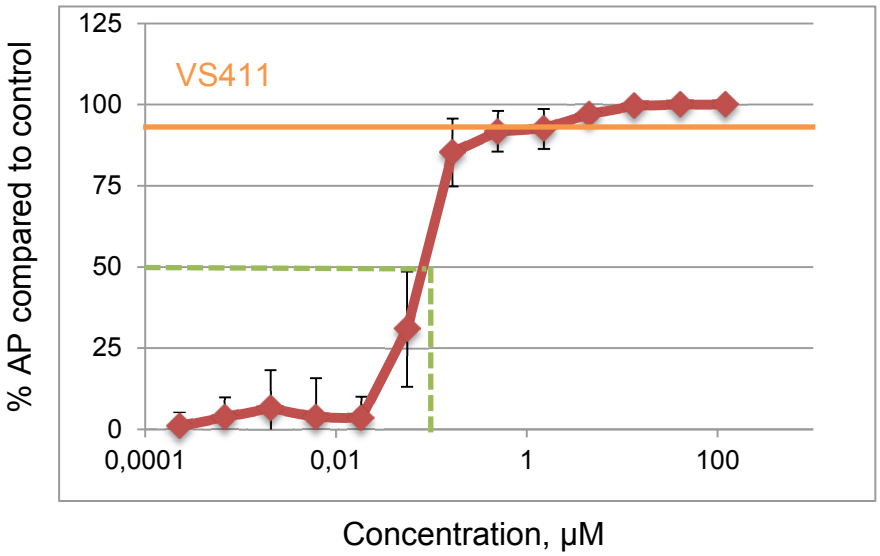

VS411 (100 µM HU/2 µM ddI) inhibited cell proliferation of 90%. VS1 had a strong antiproliferative effect with an AP_{50} value of 0.1 µM.

4.6. Determination of antiviral effect

Effect on HIV replication was assessed in resting/stimulated CD4+ cells infected with a laboratory strain of HIV-1 and exposed to different concentrations of compounds for 10 days. Viral replication was measured at the end of the experiment through determination of levels of protein p24 by ELISA. Antiviral activity (AV) was calculated as 100 minus the % p24 compared to the control (AV of control = 0%). AV_{50} was calculated by interpolation of the dose-response curve with the final goal to identify those compounds more active in inhibiting HIV replication. An example of antiviral activity dose-response curve is shown in Figure 7 below.

VS411 anti-HIV activity is shown by the orange line (90% inhibition of virus replication compared to control).

Figure 7. Determination of antiviral activity of the compound VS1

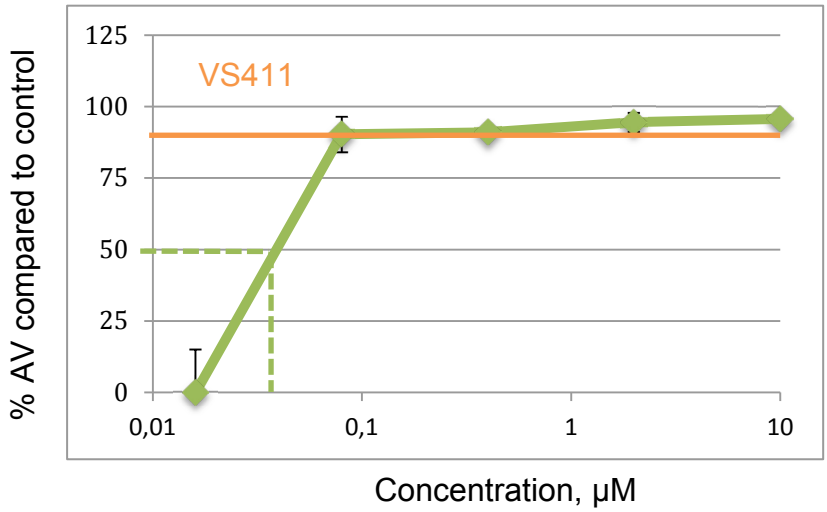

VS411 (100 μM HU/2 μM ddI) showed a 90% inhibition of viral replication. VS1 strongly inhibited HIV replication with an AV_{50} of 0.03 μM.

4.7. Identification of hit compounds

All the parameters calculated along the screening of the library of CDK9 inhibitors were employed to identify those compounds to be moved ahead in the preclinical development.

Below is a table listing three promising candidates (hits) identified during the initial screening.

Table 2. Hit compounds

	Cytotoxicity	Antiproliferative Activity	Antiviral Activity	Mitochondrial Toxicity	Apoptotic effect
Compound	TD_{50} (μM)	AP_{50} (μM)	AV_{50} (μM)	MTI_{50} (μM)	IC_{50} (μM)
VS12	4	0.05	0.05	>1.5	>10
VS18	20	0.07	0.15	>1.5	15
VS23	8.5	0.08	0.06	>1.5	10

Therapeutic indexes (or windows) were calculated and used to select the most active and safe compounds.

TI (AP) = TD_{50}/AP_{50}

TI (AV) = TD_{50}/AV_{50}

Table 3. Therapeutic indexes

Compound ID	TI (AP)	TI (AV)
VS12	80	80
VS18	286	133
VS23	106	142

4.8. Clinical candidate selection

The compounds were tested for preliminary ADME characteristics such as solubility, metabolic stability, CYP450 inhibition and permeability in Caco-2 cells.

This class of compounds showed poor solubility in aqueous ambient (about 1 μM in phosphate buffer pH 7.4 as per thermodynamic solubility determination).

Metabolic stability of the test compounds was assayed in microsomes from different species.

Table 4. Metabolic stability

Compound ID	Rat Clearance (μL/min/mg protein)	Human Clearance (μL/min/mg protein)
VS12	84.5 ± 3.25	64.4 ± 0.85
VS18	586.4 ± 11.9	115.2 ± 0.1
VS23	745.7 ± 2.4	89.6 ± 4.0

The three compounds showed high levels of clearance i.e. drug metabolism through liver microsomes was quite elevated, thus indicating a low metabolic stability of the

drugs.

Inhibition of the most important CYP450 isoforms (CYP1A2, CYP2C9, CYP2C19, CYP2D6, CYP3A4) was measured in specific assays, using specific substrates that become fluorescent upon CYP metabolism.

Table 5. CYP450 inhibition

	CYP1A2	CYP2C9	CYP2C19	CYP2D6	CYP3A4
Compound ID	% inhibition at 10 μM				
VS12	60	79	43	<5	19
VS18	80	<5	80	<5	80
VS23	80	40	80	<5	70

Compounds VS18 and VS23 had some effect on CYP1A2, CYP2C19 and CYP3A4. Compound VS12 inhibited CYP1A2 and CYP2C9.

The intestinal permeability of compounds was evaluated in the human Caco-2 model, in which the flux of the test compound from the apical (A) to the basolateral (B) side (together with B to A) is measured in order to predict the absorption from the lumen of the gut.

Table 6. Permeability determination

Compound	A→B Mass balance Mean %	B→A Mass balance Mean %	BA/AB Ratio
VS12	39	35	0.9
VS18	65	99	1.1
VS23	94	109	0.8

Permeability of the three compounds was good.

In the attempt to increase metabolic stability of the compounds the three hits were chemically modified in order to originate three different families of compounds and to be able to identify an optimized lead compound with improved ADME properties. The nature of the chemical modifications can not be revealed in this thesis due to intellectual property constraints.

The newly synthesized compounds were retested through the screening platform in order to detect activity and toxicity profiles of the compounds.

Table 7. Activity and toxicity profiles of newly synthesized compounds

Compound ID	AV_{50}	AV_{90}	AP_{50}	TD_{50}	TI_{50} (AV)	TI_{90} (AV)	TI_{50} (AP)
VS12-A	0,04	0,3	0,08 (EST)	15	375	50	187 (EST)
VS12-B	0,003(EST)	0,1	<0,08	7	2333	70	>87
VS12-C	<0,003	0,05	0,03	5	>1667	100	167
VS12-D	<0,003	0,08	0,09 (EST)	12	>4000	150	133
VS12-E	<0,003	0,4	0,04	10	>3333	25	250
VS12-F	0,016	0,4	>0,08	15	938	38	<187
VS18-A	0,03	0,4	0,05	15	500	38	300
VS18-B	0,03	0,4	<0,08	20 (EST)	667	50	>250
VS18-C	0,008	0,02	<0,08	5	625	250	>62
VS18-D	0,01	0,03	<0,08	10	1000	333	>125

Compound ID	AV_{50}	AV_{90}	AP_{50}	TD_{50}	TI_{50} (AV)	TI_{90} (AV)	TI_{50} (AP)
VS18-E	<0,003	<0,003	-	6	>2000	>2000	-
VS18-F	<0,08	<0,08	-	4	>50	>50	-
VS18-G	0,008	0,05	<0,08	15	1875	300	>187
VS18-H	0,06 (EST)	0,3	-	3 (EST)	50	10	-
VS18-I	0,007	0,04	-	12	1714	300	-
VS18-L	0,06	>0,4	-	12	200	<30	-
VS18-M	0,1	>0,4	-	4	40	<10	-
VS23-A	0,25	>0,4	-	>20	>80	>50	-
VS23-B	0,2	0,6	-	10	50	17	-
VS23-C	0,08	0,4	-	>2	>25	>5	-
VS23-D	0,05	0,4	-	7	140	18	-

Compounds were also tested for ADME properties determination and again the following parameters were examined: permeability in Caco-2 cells, metabolic stability and CYP450 inhibition profile.

Table 8. ADME parameters of the newly synthesized compounds

	Caco-2, 10 μM, pH 6,5/7,4		Metabolic stability, Clint (microsomes)		CYP450 % inhibition of control values @10μM				
Compound ID	AB perm. (10^{-6}cm/s)	BA perm. (10^{-6}cm/s)	human	rat	1A2	2C9	2C19	2D6	3A4
VS12-A	49	22	183	<115,5	57	28	35	8	38
VS12-B	46	27	<115,5	<115,5	66	26	28	5	32
VS12-C	61	27	<115,5	<115,5	37	31	45	11	41
VS12-D	60	29	<115,5	<115,5	21	17	19	4	30
VS12-E	46	36	<115,5	<115,5	29	20	30	10	46
VS12-F	46	26	<115,5	119	26	38	62	5	44
VS18-A	55	23	411	<115,5	70	28	71	3	80
VS18-B	72	17	501	<115,5	84	28	78	23	82
VS18-C	51	15	625	<115,5	81	46	80	7	84
VS18-D	53	9	744	216	93	48	90	45	87
VS18-E	59	12	949	148	85	47	84	19	88
VS18-F	48	19	268	897	78	59	88	21	88
VS18-G	83	20	535	<115,5	75	21	90	0	82
VS18-H	76	8	550	<115,5	50	23	52	9	55

	Caco-2, 10 µM, pH 6,5/7,4		Metabolic stability, Clint (microsomes)		CYP450 % inhibition of control values @10µM				
Compound ID	AB perm. (10^{-6}cm/s)	BA perm. (10^{-6}cm/s)	human	rat	1A2	2C9	2C19	2D6	3A4
VS18-I	62	17,7	390,1	<115,5	83	44	74	9	82
VS18-L	52,8	7,9	1168,8	561,2	85	31	88	24	79
VS18-M	72,8	26	767,7	148,1	61	32	86	37	94
VS23-A	50,9	16,5	356,4	<115,5	57	21	68	9	32
VS23-B	34,7	9,8	477,4	<115,5	62	29	78	8	62
VS23-C	35	13,8	417,6	<115,5	82	44	88	38	71
VS23-D	<0,4	0	-	-	50	15	74	8	22

Compounds VS12-C, VS12-E and VS12-F showed promising ADME parameters (good permeability, metabolic stability and CYP450 inhibition profile) and were selected for a preliminary *in vivo* experiment in rodents aimed at determining the oral bioavailability of the compounds and selecting a clinical candidate compound to be moved ahead in development.

Table 9. Pharmacokinetic parameters after intravenous administration of the compounds

IV administration 3 mg/kg, 3 rats per compound							
Compound ID	**$T_{1/2}$ min**	**MRT last**	**CL ml/min/kg**	**Vz, volume of distribution, ml/kg**	**Vss, estimated volume of distribution at steady state, ml/kg**	**AUC_{last} min*ng/ml**	**AUC_{inf} min*ng/ml**
VS12-C	48	18	47	3231	917	42743	42907
VS12-E	109	26	27	4109	908	73494	74468
VS12-F	134	23	46	9139	1420	45740	46181

Table 10. Pharmacokinetic parameters after oral administration (PO) of the compounds.

PO administration, 10 mg/kg, 3 rats per condition							
Compound ID	**FPO**	**T_{max} min**	**C_{max} ng/mL**	**$T_{1/2}$ min**	**MRT_{last} min**	**AUClast min*ng/ml**	**AUCinf min*ng/ml**
VS12-C	63	30	1482	31	68	135368	136834
VS12-E	42	30	2211	26	60	154169	154343
VS12-F	36	30	1004	119	113	81328	82372

Compound VS12-C resulted to be the compound with better bioavailability (FPO, the fraction of the administered compound that reaches systemic circulation) compared to the other ones. This compound had also a promising activity/toxicity profile, as shown below.

Figure 8. Activity and toxicity profiles of compound VS12-C

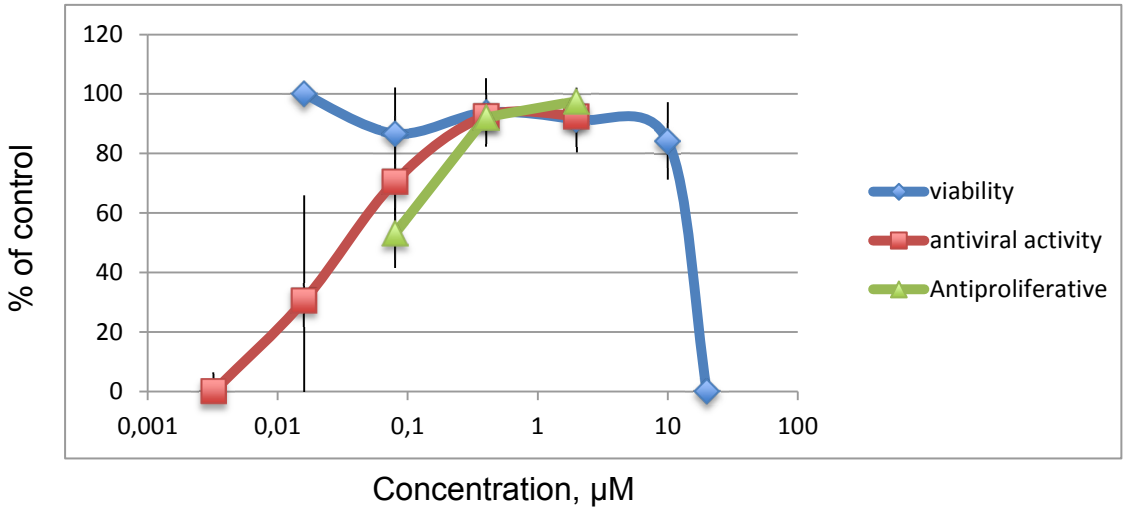

Compound VS12-C had a good activity and toxicity profile with optimal therapeutic indexes. This compound was moved forward into preclinical development to further *in vivo* studies to determine tolerability and toxicokinetic profile.

4.9. Preliminary toxicology study

Aim of this study was to collect preliminary information on the toxic profile of compound VS12-C after single oral treatment at 500 mg/kg (formulated as a suspension) and after 5-day repeated treatment at 100 mg/kg (formulated as a solution) in the mouse. The mouse was chosen in order to use a small amount of compound in this preliminary test. Satellite groups were also treated in parallel in order to evaluate the plasma exposure after the administration of 500 mg/kg in suspension and prior and after the fifth day of treatment at 100 mg/kg.

During the repeated 5-day treatment at 100 mg/kg/day no relevant clinical signs and no mortality were observed during the whole treatment. No statistically significant differences were found within weights of the vehicle and the treated groups of animals.

Figure 9. Average weights during the 8 days of observation

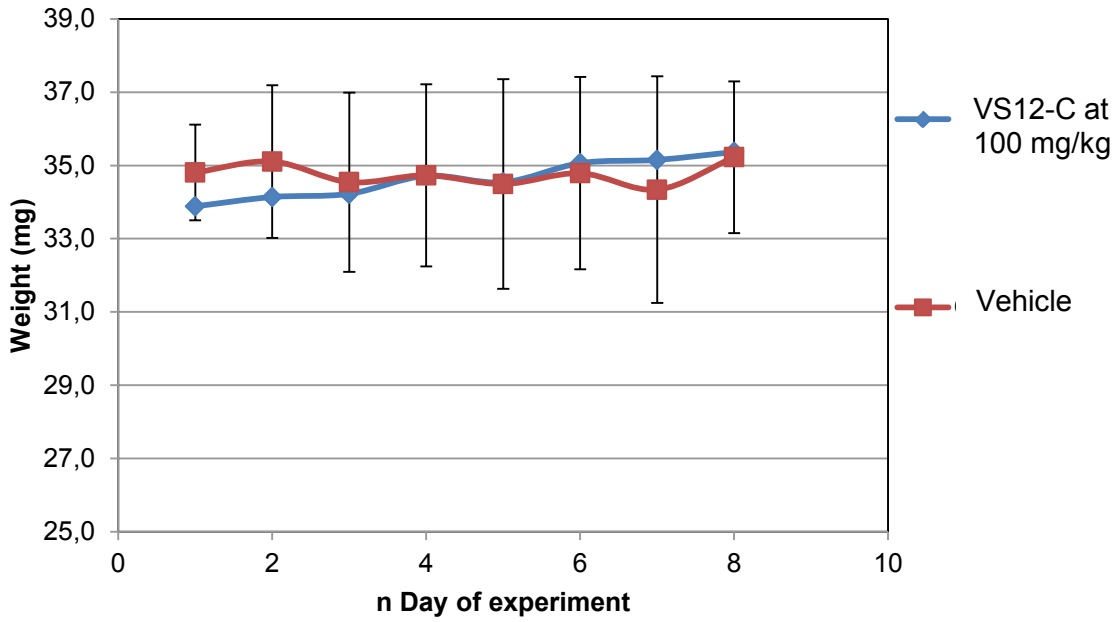

After acute treatment at 500 mg/kg three animals were found dead 24 hrs after compound administration. Two animals were sacrificed in extremis 24 hrs after the compound administration because they were in pre-agonic status. The necroscopy performed on these animals indicated gastric problems with a moderated to severe presence of coagulated blood in stomachs.

Plasma of the satellite groups were analysed to correlate the toxicological effects.

No significant accumulation of the compound was found after administration of 100 mg/kg for 5 days. Some variability was noted within the subjects.

Figure 10. Average plasma exposure after oral gavage at 100 mg/kg as a solution

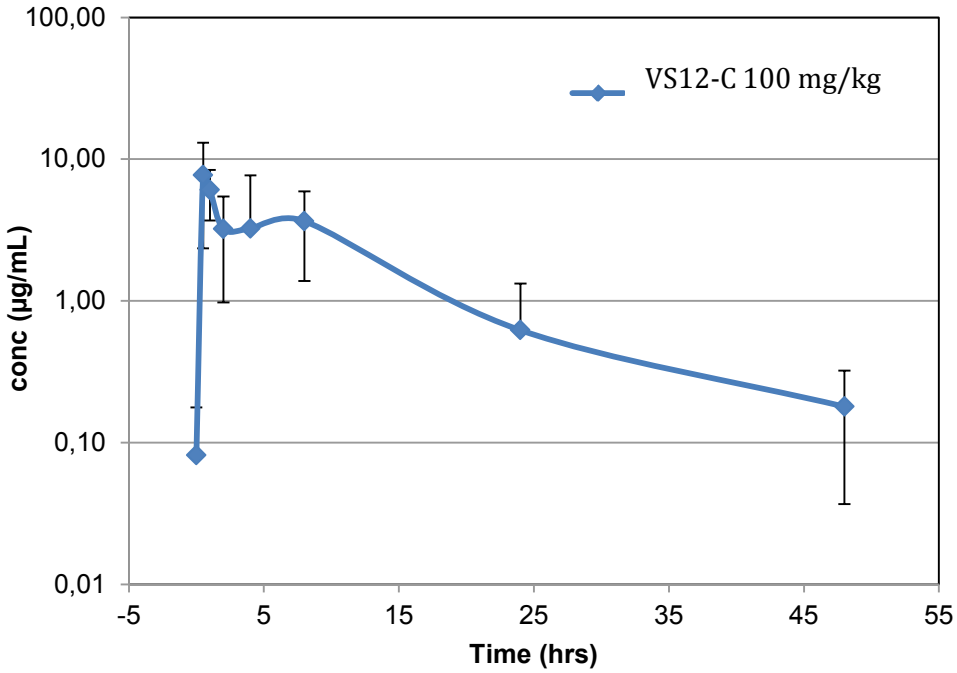

Pharmacokinetic parameters are reported in Table 11.

Table 11. Pharmacokinetic parameters of VS12-C after 5 days repeated treatment at 100 mg/kg

PO 100 mg/Kg	Mean	SD
$T_{1/2}$ (hr)	7.92	1.00
T_{max} (hrs)	1.67	2.02
C_{max} (µg/ml)	8.77	4.92
T_{last} (hrs)	48	-
C_{last_obs} µg/ml	0.18	0.71
AUC_{0-t} (µg/ml*hr)	74.03	33.68
MRT_{0-inf} (hr)	11.69	3.23

A large exposure variability was found within the subjects treated with the suspension at 500 mg/kg (Figure 11) and plasma levels showed an erratic exposure probably due to the precipitation and re-dissolution of the compound after oral gavage.

Figure 11. Average plasma exposure after oral gavage at 500 mg/kg as suspension

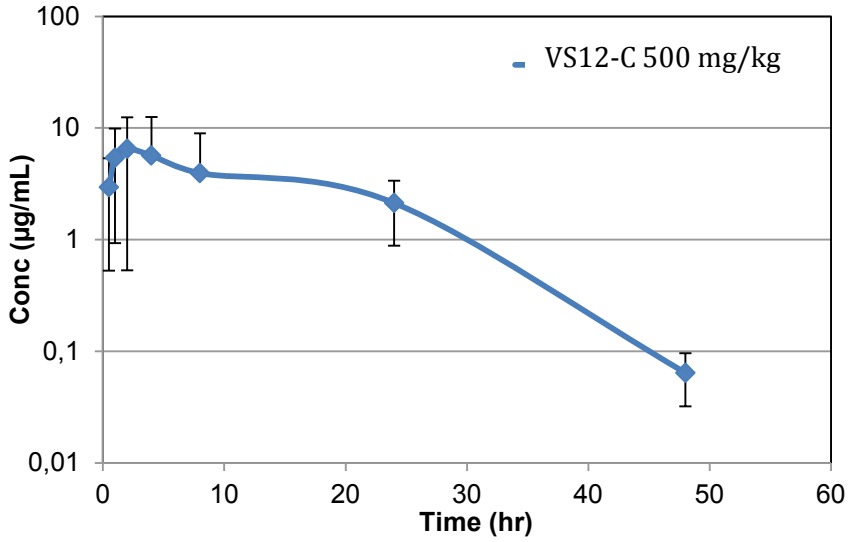

Pharmacokinetic parameters are reported in Table 12.

Table 12. Pharmacokinetic parameters for single treatment at 500 mg/kg

PO 500 mg/Kg	Mean	SD
$T_{1/2}$ (hrs)	6.46	0.78
T_{max} (hrs)	7.20	9.44
C_{max} (µg/ml)	7.08	5.82
T_{last} (hrs)	40.8	17.2
C_{last_obs} µg/ml	0.06	0.03
AUC_{0-t} (µg/ml*hrs)	74.03	33.68
MRT_{0-inf} (hrs)	11.69	3.23

As it can be observed from Figure 12 exposure at 500 mg/kg was comparable with that achieved at 100 mg/kg therefore the toxicological effects could not be attributed to a systemic exposure but probably to a local toxicity due to the precipitation of the compound in the stomach. Ratio between the AUC at 500 and 100 mg/kg is only 1.35 confirming a better exposure of the solution compared to the tested suspension.

Figure 12. Comparison between exposure after single oral gavage at 100 mg/kg and 500 mg/kg

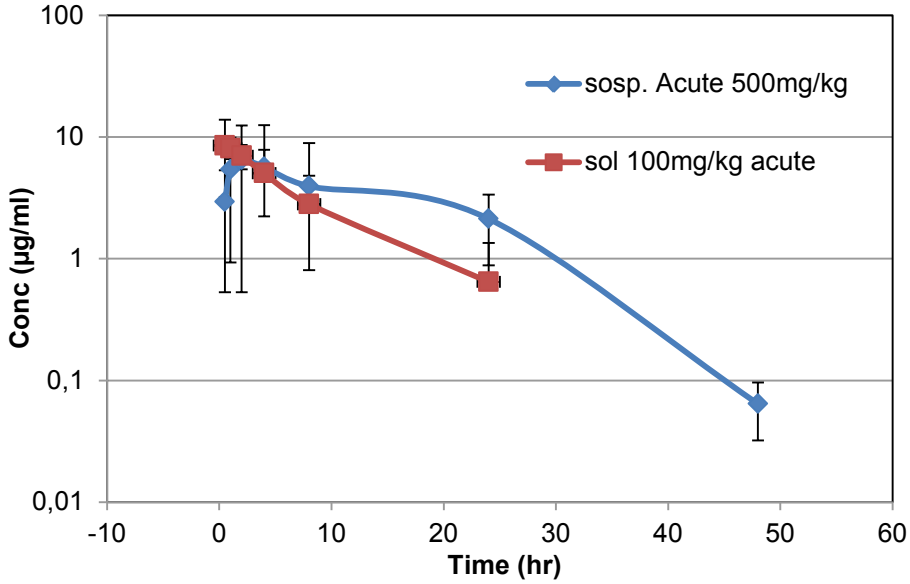

4.10. Activity against other viruses

CDK9 is involved in the life cycle of viruses other than HIV so it was decided to test the activity of a representative set of compounds against a panel of different viruses to explore potential activity of CDK9 inhibitors.

Table 13. Activity of compounds against Herpes virus type 1 and 2

	HSV-1			HSV-2		
Compound	EC_{50} µM	CC_{50}	SI_{50}	EC_{50} µM	CC_{50}	SI_{50}
Acyclovir	2.9	>100	>35	3.9	>100	>26
VS1	>100	>100	1.0	>100	>100	1.0
VS2	>20	89.1	<4	>20	89.1	<4
VS3	>20	89.4	<4	>20	89.4	<4
VS4	>20	43.3	<2	>20	43.3	<2
VS5	>20	78.2	<4	>20	78.2	<4
VS6	>20	91.5	<5	>20	91.5	<5
VS7	>20	72.9	<4	>20	72.9	<4
VS8	>20	96.5	<5	>20	96.5	<5
VS9	0.6	54.4	91.0	3.2	54.4	17.0
VS10	>20	71.6	<4	>20	71.6	<4
VS11	>20	87.3	<4	>20	87.3	<4
VS12	>20	88.9	<4	>20	88.9	<4
VS13	>100	>100	1.0	>100	>100	1.0
VS14	>100	>100	1.0	>100	>100	1.0
VS15	>4	19.8	<5	>4	19.8	<5
VS16	>4	19.9	<5	>4	19.9	<5
VS17	>20	59.2	<3	>20	59.2	<3
VS18	>20	95.3	<5	>20	95.3	<5

Compound VS9 resulted very active against both HSV-1 and HSV-2 with a selectivity index (SI_{50}=CC_{50}/EC_{50}) of 91 and 17 for the two viruses, respectively.

Compounds were also tested against EBV, results are described in the following table.

Table 14. Activity against Epstein-Barr Virus

	EBV		
Compound	EC_{50} µM	CC_{50}	SI_{50}
Acyclovir	17.4	>100	>6
VS1	0.5	1.1	2.0
VS2	<0.48	<0.48	1.0
VS3	<0.48	<0.48	1.0
VS4	>0.48	2.0	<4
VS5	>2.40	2.6	<1
VS6	<0.48	<0.48	1.0
VS7	4.8	11.5	2.0
VS8	1.2	8.1	8.0
VS9	>0.48	1.0	<2
VS10	0.7	2.0	3.0
VS11	>2.40	9.2	<4
VS12	7.7	11.0	1.0
VS13	>12	26.0	<2
VS14	>2.40	6.1	<3
VS15	2.8	6.5	2.0
VS16	<0.48	7.9	>16
VS17	0.9	2.2	2.0
VS18	>2.40	6.6	<3

Compounds VS8 and VS16 were active against EBV with good selectivity indexes.

Activity of CDK9 inhibitors against HPV was assayed, results are depicted in the following table.

Table 15. Activity of CDK9 inhibitors against Human Papilloma Virus

	HPV				
Compound	EC_{50} µM	EC_{90}	CC_{50}	SI_{50}	SI_{90}
Cidofovir	148.0	>200	>200	>1	>1
VS1	33.2	>100	>100	>3	1.0
VS2	11.5	>100	>100	>9	1.0
VS3	48.7	>10	85.8	2.0	<9
VS4	1.7	20.0	>100	>60	>5
VS5	26.7	54.8	>100	>4	>2
VS6	9.7	14.0	>100	>10	>7
VS7	>100	>100	>100	1.0	1.0
VS8	1.8	41.7	>100	>54	>2
VS9	9.4	28.9	35.9	4.0	1.0
VS10	29.1	43.4	49.9	2.0	1.0
VS11	0.5	90.8	>100	>185	>1
VS12	39.0	90.2	>100	>3	>1
VS13	16.7	55.4	>100	>6	>2
VS14	28.6	48.1	>100	>4	>2
VS15	>1	>1	8.3	<8	<8
VS16	17.2	35.3	>100	>5	>3
VS17	0.3	40.8	>100	>323	>3
VS18	9.9	30.4	>100	>10	>3

Compounds VS2, VS4, VS8, VS11, VS17 and VS18 were strongly active against HPV with SI_{50} values of >9, >60, >54, >185, >323 and >10, respectively.

4.11. Activity against cancer cell lines

The antiproliferative effect of selected CDK9 inhibitors was investigated *in vitro* in the following cancer cell lines: A2780 (Ovarian cancer), H1299 (Lung cancer), MNK45 (Gastric cancer), HEC1A (Endometrial cancer) and Jurkat (T cell leukemia).
Dose-response curves (mean of two experiments) of five selected compounds were obtained for each cancer cell line.

Figure 13. Dose-response curves for the different cancer cell lines

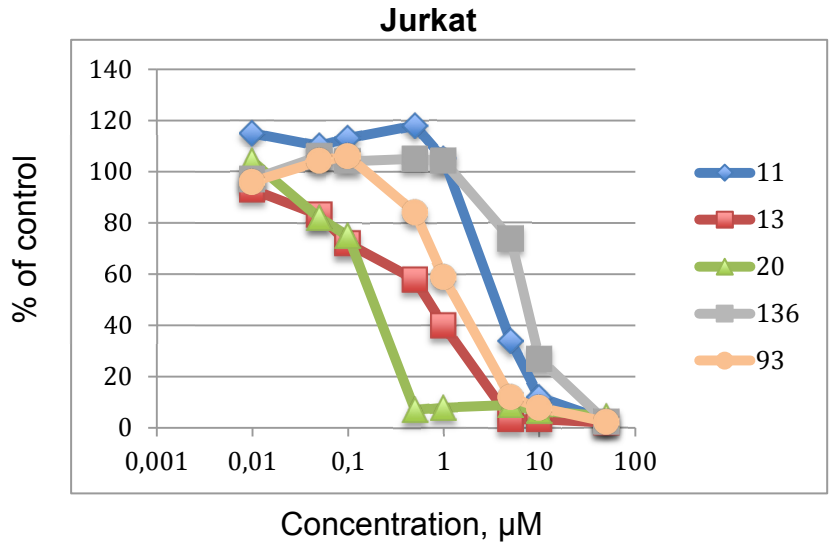

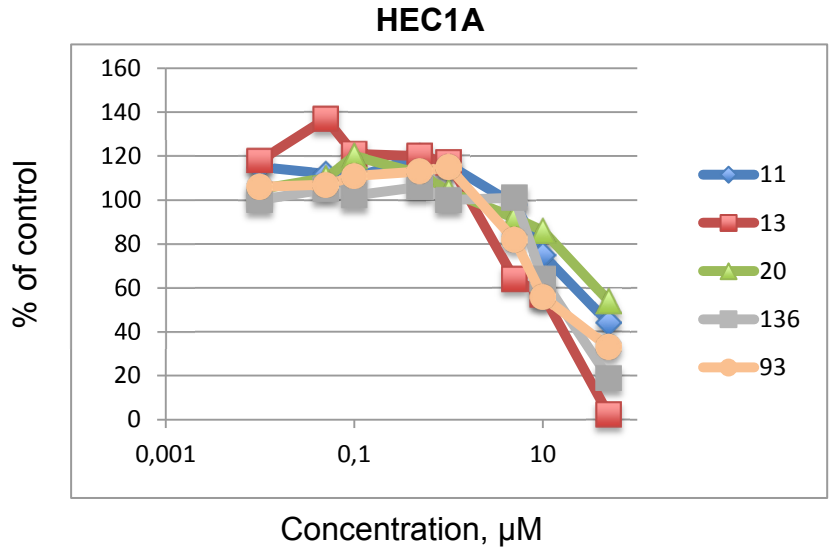

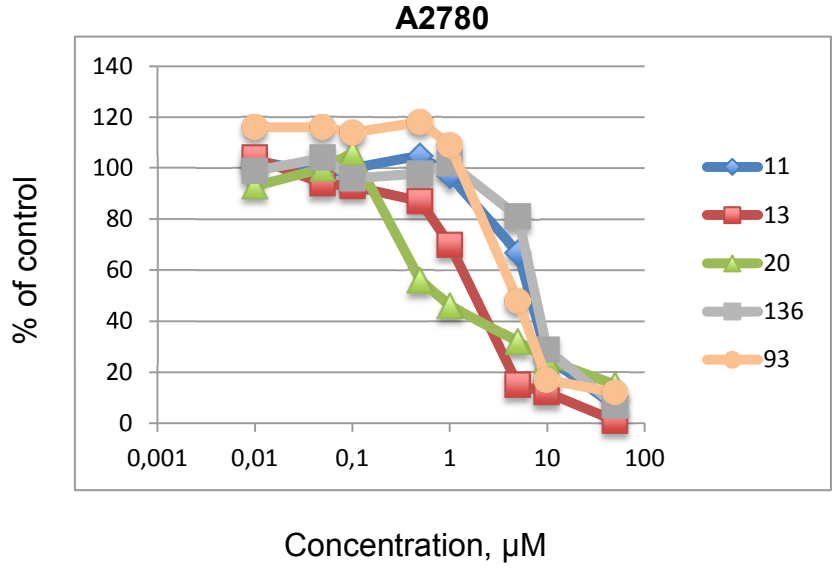
A2780
% of control
140
120
100
80
60
40
20
0
0,001
0,01
0,1
1
10
100
11
13
20
136
93
Concentration, μM

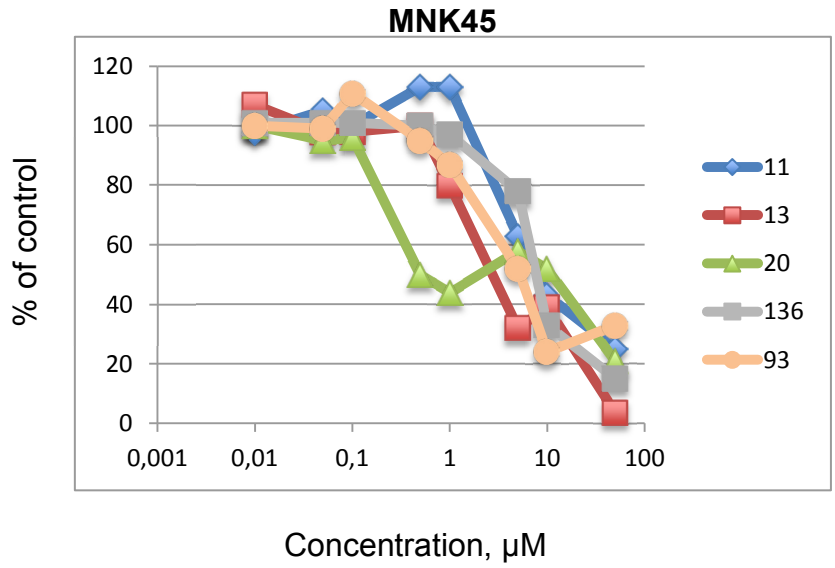
MNK45
% of control
120
100
80
60
40
20
0
0,001
0,01
0,1
1
10
100
11
13
20
136
93
Concentration, μM

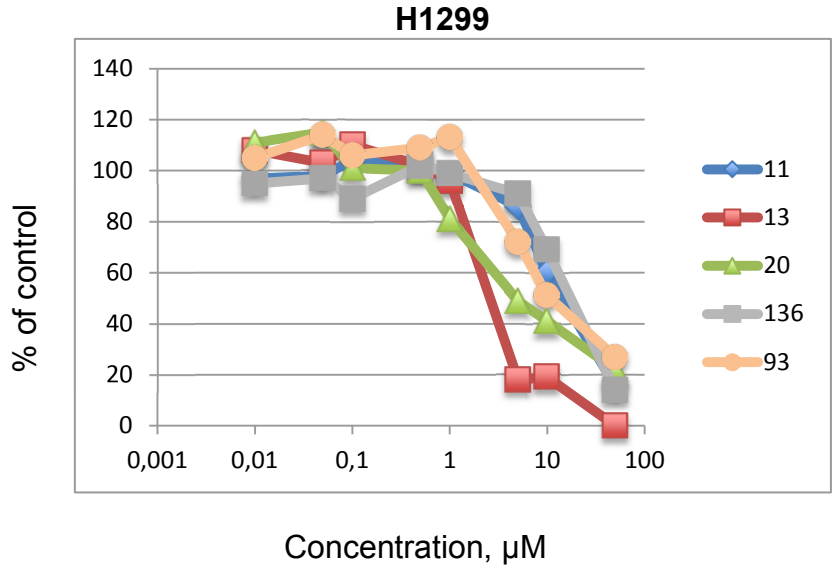
H1299
% of control
140
120
100
80
60
40
20
0
0,001
0,01
0,1
1
10
100
11
13
20
136
93
Concentration, μM

A summary of the IC_{50} values obtained through the interpolation of the dose-response curves of two different experiments is shown in the following table.

Table 16. Summary of the IC_{50} values of the compounds analyzed in the five cancer cell lines

Compound ID	CDK9 IC_{50} nM	A2780 (Ovarian Cancer)	H1299 (lung cancer)	MNK45 (Gastric Cancer)	HEC1A (Endometrial Cancer)	Jurkat (T Cell Leukemia)
VS11	54	7.0555	27.175	8.461	43.15	5.161
VS13	17	2.7965	5.683	7.9665	23.95	1.8
VS20	26	0.46	17.1	8	52.1	0.255
VS93	56	6.2	15.2	6.19	25.9	1.955
VS136	46	7.8815	35.3	8.14	22.283	7.705

The clinical candidate for the HIV/AIDS program VS12-C was also tested in lung cancer cell line (H1299) and proved to be active in inhibiting tumor cell line proliferation.

Figure 14. Dose-response curve of compound VS12-C

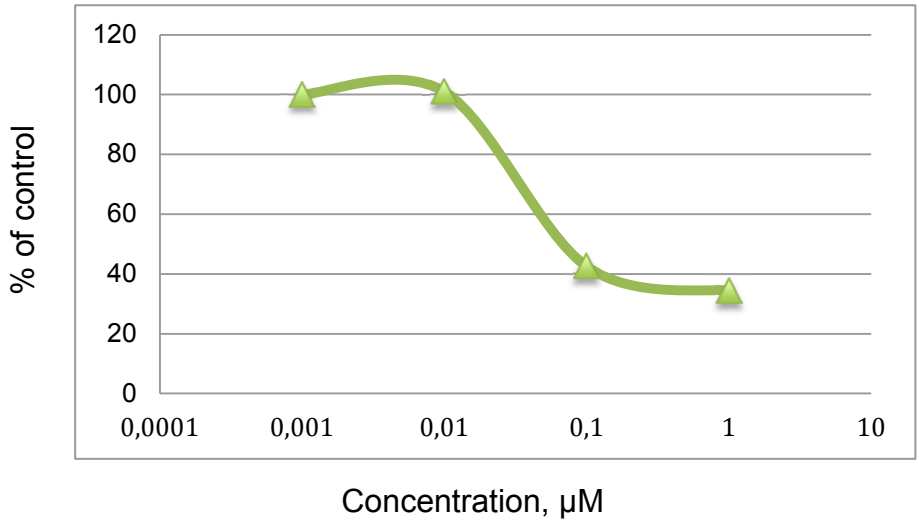

IC_{50} towards H1299 for compound VS12-C was found to be 0.07 µM.

4.12. Activity in mouse xenograft model of lung cancer

Compound VS12-C was tested in a lung cancer (H1299) mouse xenograft model. The experiment was performed in collaboration with Mario Negri Institute (Milan). Athymic female mice were injected with a cell suspension containing H1299 cells, when tumor load reached the proper size mice were randomized to receive vehicle (5% NMP, 85% PEG400, 10% water) or compound at 50 mg/kg/day by oral administration. Tumor size and mouse body weight were recorded three times a week from treatment start until the end of the study after 15 days of treatment.
Treatment was well tolerated with apparent no signs of toxicity.

Figure 15. Body weight

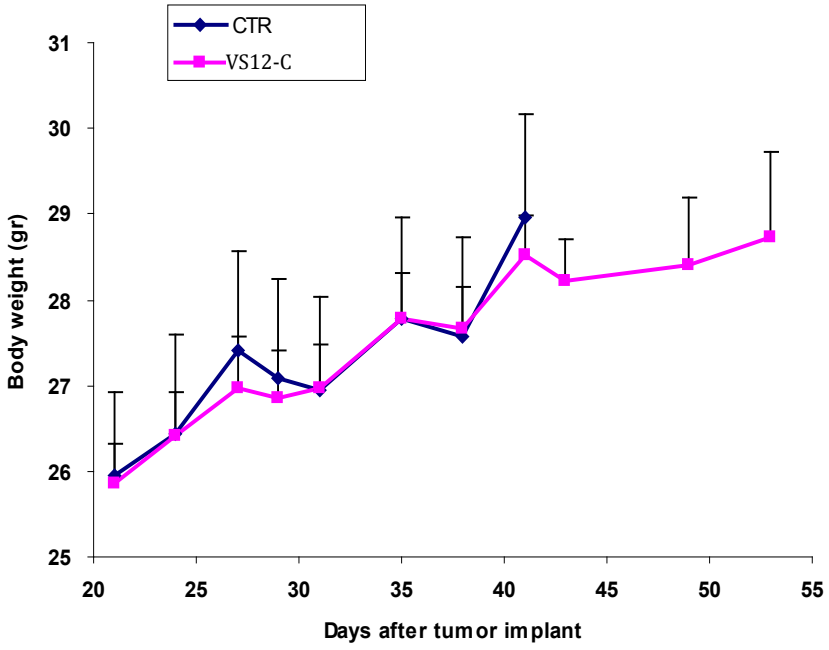

Figure 16. Tumor size

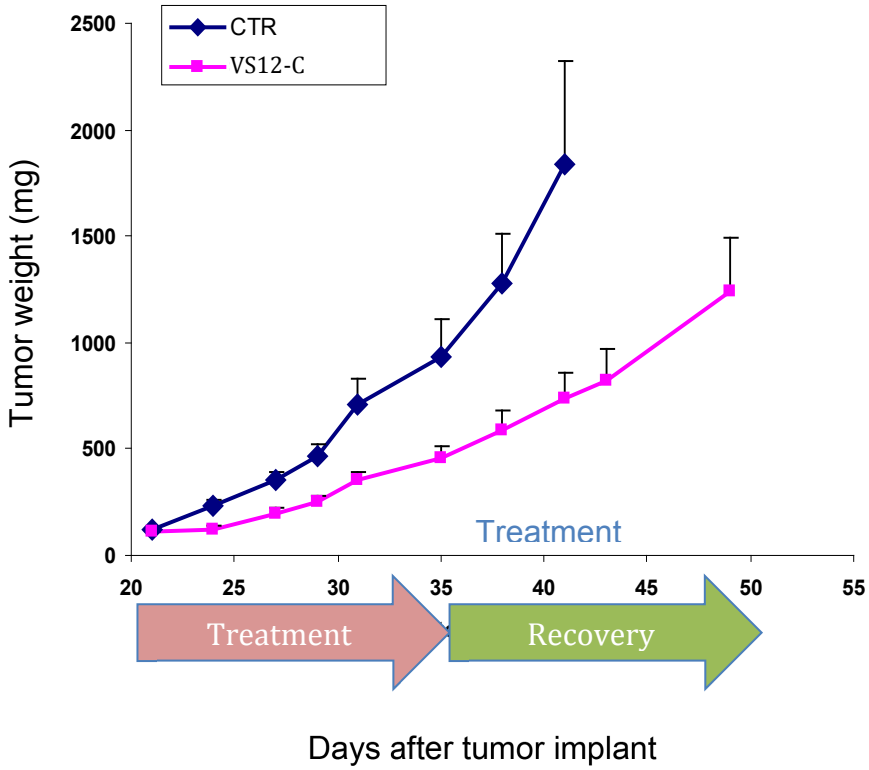

A growth inhibitory effect on the tumor mass was observable.

After treatment cessation (Day 35 from tumor implant) the curve inclination in the treated animals was still diverging from the controls.

5. DISCUSSION

Immune system hyperactivation/hyperproliferation/inflammation occurs most rapidly and to the greatest extent in HIV/AIDS. Upon infection by HIV, it is actually the subsequent uncontrolled immune system hyperactivation that ultimately results in immune exhaustion, loss of $CD4^+$ T helper cells, accelerated senescence (aging), cardiovascular and other organ diseases, and, consequently, the onset of AIDS. The chronic level of excessive inflammation seen in HIV is now recognized as a primary driver of a growing number of “non-AIDS defining events” that negatively affect both quality of life and life expectancy in HIV-infected individuals. These include cardiovascular diseases (including strokes and heart attacks), inflammatory and metabolic disorders, as well as liver, kidney and CNS disease, bone loss, and increased rates of cancer. Advances in HIV drug therapy today allow most patients to reduce the amount of virus in their bloodstreams to undetectable levels by use of antiretroviral treatment (ART) multi-drug cocktails. Despite the ability of such anti-HIV cocktails to effectively reduce viremia, HIV patients still progress to AIDS and continue to suffer a reduced life expectancy due to a number of diseases resulting from uncontrolled immune system hyperactivation. The possibility of reducing both immune hyperactivation and viral load in HIV-infected subjects has been proven by the first AV-HALT drug, VS411 (originally developed by ViroStatics), an experimental combination of two registered drugs that has provided essential human Proof of Concept for this new class of drugs. Focus of the work was then to identify AV-HALT compounds combining antiviral and antiproliferative activity in a single molecule. These compounds possess a novel antiviral mechanism of action compared to traditional ARVs used in combination regimens currently on the market, i.e. targeting a human rather than a viral enzyme. Such compounds have been identified upon testing libraries of inhibitors of CDK9, which has been reported as essential for HIV-1 replication and also involved in cell proliferation. CDK9 in complex with cyclin T1 is involved in viral genes transcription as it promotes processivity of RNAPII and is also involved in cell proliferation as its kinase activity is involved in promoting recovery from replication arrest in stress responses at the G2/M check point (Zhang 2013).

By testing toxicity, antiproliferative capacity and antiviral activity of compounds, a number of AV-HALT "drug hits" (compounds with the desired *in vitro* AV-HALT profile) having optimal therapeutic indexes have been identified. Such compounds, belonging to similar but distinct classes of molecules, share AV-HALT properties similar to the "proof-of-concept" reference standard VS411, making them suitable for drug development.

A crucial part of the project was focused on the preclinical development of the compounds. Different ADME parameters have been evaluated to select not only compounds that are active *in vitro* but also compounds that are suitable for drug development. In particular, the following sets of data were pursued:

a) Investigation of the potential of AV-HALT compounds to inhibit human CYP450 activity *in vitro*, evaluating the CYP450 interaction of such compounds with the five most important isoforms enzyme;

b) Investigation of AV-HALT compound clearance with liver microsomes, evaluating the metabolic stability of such compounds in rat and human liver microsomes in order to estimate stability to phase I oxidative metabolism;

c) Caco-2 permeability assessment to investigate possible efflux phenomena;

d) Solubility studies.

The first hit compounds had some drawbacks, mainly dealing with the low metabolic stability. This means that the drug candidates may have the potential to form undesired, potentially toxic, or pharmacologically inactive/active metabolites. The issue has been addressed and solved by inserting some chemical modifications (substituents) in order to improve metabolic stability of the compounds.

We also learnt that solubility is an important issue for this class of CDK9 inhibitors. It is generally desirable for a drug molecule to have some level of water solubility. These compounds showed very poor solubility in acqueous ambient (about 1 μM in phosphate buffer pH 7.4). Low solubility can translate into poor and varying bioavailability, can slow down the overall development process, can lead to increased development costs and to the development of a suboptimal drug for the

patient. Poor water solubility can be addressed with a good formulation work. In fact we are already developing a new formulation to improve solubility and increase drug exposure *in vivo*. An excellent enabling formulation strategy is the nanosizing (e.g., wet bead milling) technology. Drug nanocrystal technology has emerged in the last 15-20 years mainly due to the benefits that can be gained by formulating poorly soluble drugs. This approach generally produces dispersions of drug nanocrystals in a liquid medium (typically water), which are called “nanosuspensions”. Nanosuspensions consist essentially of pure drug nanoparticles (100–1000 nm) and a minimum amount of surface active agents and polymers required for stabilization. This technology can significantly enhance the effective surface area of the drug, thus resulting in increased exposure.

Through the *in vitro* screening platform and several rounds of ADME parameters characterization we were able to improve the activity and druggability characteristics of the molecules. We have now identified a lead second generation AV-HALT with optimal activity and toxicity profile *in vitro*, with promising ADME properties and good oral bioavailability. Further studies are underway to complete VS12-C preclinical development and better elucidate the mechanism of action.

CDK9 as a cellular factor is involved in life cycle of many other pathogens. There was a good rationale to test activity of CDK9 inhibitors against other viruses such as HSV-1/2, EBV and HPV. Several compounds have been identified that strongly inhibited replication of these viruses with a good therapeutic window. It will be important to explore the molecular mechanisms responsible for the activity.

Deregulation of cyclin-dependent kinases has been associated with many cancer types and has evoked an interest in chemical inhibitors with possible therapeutic benefit. Recently work highlighted CDK9 as a critical target responsible for the activity of several drugs currently under clinical development. We tested our library of CDK9 inhibitors and found several compounds active in vitro against several cancer cell lines. In particular compound VS12-C proved to possess good

anticancer activity both *in vitro* and *in vivo* in a mouse xenograft model of lung cancer.

6. REFERENCES

Baker JV, Peng G, Rapkin J, Krason D, Reilly C, Cavert WP, Abrams DI, MacArthur RD, Henry K, Neaton JD; Terry Beirn Community Programs for Clinical Research on AIDS (CPCRA). Poor initial $CD4^+$ recovery with antiretroviral therapy prolongs immune depletion and increases risk for AIDS and non-AIDS diseases. J Acquir Immune Defic Syndr. 2008; 48(5): 541-546.

Bark-Jones SJ, Webb HM, West MJ. EBV EBNA 2 stimulates CDK9-dependent transcription and RNA polymerase II phosphorylation on serine 5. Oncogene. 2006; 25(12): 1775-85.

Bettayeb K, Baunbæk D, Delehouze C, Loaëc N, Hole AJ, Baumli S, Endicott JA, Douc-Rasy S, Bénard J, Oumata N, Galons H, Meijer L. CDK Inhibitors Roscovitine and CR8 Trigger Mcl-1 Down-Regulation and Apoptotic Cell Death in Neuroblastoma Cells. Genes Cancer. 2010; 1(4): 369-380.

Brasier AR, Tian B, Jamaluddin M, Kalita MK, Garofalo RP, Lu M. RelA Ser276 phosphorylation-coupled Lys310 acetylation controls transcriptional elongation of inflammatory cytokines in respiratory syncytial virus infection. J Virol. 2011; 85(22): 11752-11769.

Brenchley JM, Price DA, Schacker TW, Asher TE, Silvestri G, Rao S, Kazzaz Z, Bornstein E, Lambotte O, Altmann D, Blazar BR, Rodriguez B, Teixeira-Johnson L, Landay A, Martin JN, Hecht FM, Picker LJ, Lederman MM, Deeks SG, Douek DC. Microbial translocation is a cause of systemic immune activation in chronic HIV infection. Nat Med. 2006; 12(12): 1365-1371.

Cauley JA, Wu L, Wampler NS, Barnhart JM, Allison M, Chen Z, Jackson R, Robbins J. Clinical risk factors for fractures in multi-ethnic women: the Women's Health Initiative. J Bone Miner Res. 2007; 22(11): 1816-1826.

Chen R, Keating MJ, Gandhi V, Plunkett W. Transcription inhibition by flavopiridol: mechanism of chronic lymphocytic leukemia cell death. Blood. 2005; 106(7): 2513-2519.

Chen R, Wierda WG, Chubb S, Hawtin RE, Fox JA, Keating MJ, Gandhi V, Plunkett W. Mechanism of action of SNS-032, a novel cyclin-dependent kinase inhibitor, in chronic lymphocytic leukemia. Blood. 2009; 113(19): 4637-4645.

Cujec TP, Cho H, Maldonado E, Meyer J, Reinberg D, Peterlin BM. The human immunodeficiency virus transactivator Tat interacts with the RNA polymerase II holoenzyme. Mol Cell Biol. 1997; 17(4): 1817-1823.

Deeks SG, Grant RM, Wrin T, Paxinos EE, Liegler T, Hoh R, Martin JN, Petropoulos CJ. Persistence of drug-resistant HIV-1 after a structured treatment interruption and its impact on treatment response. AIDS. 2003; 17(3): 361-370.

Dickson MA, Schwartz GK. Development of cell-cycle inhibitors for cancer therapy. Curr Oncol. 2009; 16(2): 36-43.

Douek DC. Disrupting T-cell homeostasis: how HIV-1 infection causes disease. AIDS Rev. 2003; 5(3): 172-177.

Durand LO, Advani SJ, Poon AP, Roizman B. The carboxyl-terminal domain of RNA polymerase II is phosphorylated by a complex containing cdk9 and infected-cell protein 22 of herpes simplex virus 1. J Virol. 2005; 79(11): 6757-6762.

Evans TG, Bonnez W, Soucier HR, Fitzgerald T, Gibbons DC, Reichman RC. Highly active antiretroviral therapy results in a decrease in CD8+ T cell activation and preferential reconstitution of the peripheral $CD4^+$ T cell population with memory rather than naive cells. Antiviral Res. 1998; 39(3): 163-173.

Feichtinger S, Stamminger T, Müller R, Graf L, Klebl B, Eickhoff J, Marschall M. Recruitment of cyclin-dependent kinase 9 to nuclear compartments during cytomegalovirus late replication: importance of an interaction between viral pUL69 and cyclin T1. J Gen Virol. 2011; 92(Pt 7): 1519-1531.

Finkel TH, Tudor-Williams G, Banda NK, Cotton MF, Curiel T, Monks C, Baba TW, Ruprecht RM, Kupfer A. Apoptosis occurs predominantly in bystander cells and not in productively infected cells of HIV- and SIV-infected lymph nodes. Nat Med. 1995; 1(2): 129-134.

Fujinaga K, Irwin D, Huang Y, Taube R, Kurosu T, Peterlin BM. Dynamics of human immunodeficiency virus transcription: P-TEFb phosphorylates RD and dissociates negative effectors from the transactivation response element. Mol Cell Biol. 2004; 24(2): 787-795.

Gojo I, Zhang B, Fenton RG. The cyclin-dependent kinase inhibitor flavopiridol induces apoptosis in multiple myeloma cells through transcriptional repression and down-regulation of Mcl-1. Clin Cancer Res. 2002; 8(11): 3527-3538.

Gordon V, Bhadel S, Wunderlich W, Zhang J, Ficarro SB, Mollah SA, Shabanowitz J, Hunt DF, Xenarios I, Hahn WC, Conaway M, Carey MF, Gioeli D. CDK9 regulates AR promoter selectivity and cell growth through serine 81 phosphorylation. Mol Endocrinol. 2010; 24(12): 2267-2280.

Grossman Z, Meier-Schellersheim M, Paul WE, Picker LJ. Pathogenesis of HIV infection: what the virus spares is as important as what it destroys. Nat Med. 2006; 12(3): 289-295.

Grossman Z, Paul WE. The impact of HIV on naïve T-cell homeostasis. Nat Med. 2000; 6(9): 976-977.

Hahntow IN, Schneller F, Oelsner M, Weick K, Ringshausen I, Fend F, Peschel C, Decker T. Cyclin-dependent kinase inhibitor Roscovitine induces apoptosis in chronic lymphocytic leukemia cells. Leukemia. 2004; 18(4): 747-755.

Helfer CM, Yan J, You J. The cellular bromodomain protein Brd4 has multiple functions in E2-mediated papillomavirus transcription activation. Viruses. 2014; 6(8): 3228-3249.

Hellerstein MK, Hoh RA, Hanley MB, Cesar D, Lee D, Neese RA, McCune JM. Subpopulations of long-lived and short-lived T cells in advanced HIV-1 infection. J Clin Invest. 2003; 112(6): 956-966.

Ho JE, Deeks SG, Hecht FM, Xie Y, Schnell A, Martin JN, Ganz P, Hsue PY. Initiation of antiretroviral therapy at higher nadir $CD4^+$ T-cell counts is associated with reduced arterial stiffness in HIV-infected individuals. AIDS. 2010; 24(12): 1897-1905.

Hunt PW, Martin JN, Sinclair E, Bredt B, Hagos E, Lampiris H, Deeks SG. T cell activation is associated with lower $CD4^+$ T cell gains in human immunodeficiency virus-infected patients with sustained viral suppression during antiretroviral therapy. J Infect Dis. 2003; 187(10): 1534-1543.

Ivanov D, Kwak YT, Guo J, Gaynor RB. Domains in the SPT5 protein that modulate its transcriptional regulatory properties. Mol Cell Biol. 2000; 20(9): 2970-2983.

Jang MK, Mochizuki K, Zhou M, Jeong HS, Brady JN, Ozato K. The bromodomain protein Brd4 is a positive regulatory component of P-TEFb and stimulates RNA polymerase II-dependent transcription. Mol Cell. 2005; 19(4): 523-534.

Krystof V, Chamrád I, Jorda R, Kohoutek J. Pharmacological targeting of CDK9 in cardiac hypertrophy. Med Res Rev. 2010; 30(4): 646-666.

Krystof V, Uldrijan S. Cyclin-dependent kinase inhibitors as anticancer drugs. Curr Drug Targets. 2010; 11(3): 291-302.

Lam LT, Pickeral OK, Peng AC, Rosenwald A, Hurt EM, Giltnane JM, Averett LM, Zhao H, Davis RE, Sathyamoorthy M, Wahl LM, Harris ED, Mikovits JA, Monks AP, Hollingshead MG, Sausville EA, Staudt LM. Genomic-scale measurement of mRNA turnover and the mechanisms of action of the anti-cancer drug flavopiridol. Genome Biol. 2001; 2(10): RESEARCH0041.

Lapenna S, Giordano A. Cell cycle kinases as therapeutic targets for cancer. Nat Rev Drug Discov. 2009; 8(7): 547-566.

Lee DK, Duan HO, Chang C. Androgen receptor interacts with the positive elongation factor P-TEFb and enhances the efficiency of transcriptional elongation. J Biol Chem. 2001; 276(13): 9978-9984.

Lesho E. Evidence base for using corticosteroids to treat HIV-associated immune reconstitution syndrome. Expert Rev Anti Infect Ther. 2006; 4(3): 469-478.

Li LL, Hu ST, Wang SH, Lee HH, Wang YT, Ping YH. Positive transcription elongation factor b (P-TEFb) contributes to dengue virus-stimulated induction of interleukin-8 (IL-8). Cell Microbiol. 2010; 12(11): 1589-1603.

Li Q, Price JP, Byers SA, Cheng D, Peng J, Price DH. Analysis of the large inactive P-TEFb complex indicates that it contains one 7SK molecule, a dimer of HEXIM1 or HEXIM2, and two P-TEFb molecules containing Cdk9 phosphorylated at threonine 186. J Biol Chem. 2005; 280(31): 28819-28826.

Lori F, De Forni D, Katabira E, Baev D, Maserati R, Calarota SA, Cahn P, Testori M, Rakhmanova A, Stevens MR. VS411 reduced immune activation and HIV-1 RNA

levels in 28 days: randomized proof-of-concept study for antiviral-hyperactivation limiting therapeutics. PLoS One. 2012; 7(10): e47485.

Loyer P, Trembley JH, Katona R, Kidd VJ, Lahti JM. Role of CDK/cyclin complexes in transcription and RNA splicing. Cell Signal. 2005; 17(9): 1033-1051.

MacCallum DE, Melville J, Frame S, Watt K, Anderson S, Gianella-Borradori A, Lane DP, Green SR. Seliciclib (CYC202, R-Roscovitine) induces cell death in multiple myeloma cells by inhibition of RNA polymerase II-dependent transcription and down-regulation of Mcl-1. Cancer Res. 2005; 65(12): 5399-5407.

Mahalingam M, Peakman M, Davies ET, Pozniak A, McManus TJ, Vergani D. T cell activation and disease severity in HIV infection. Clin Exp Immunol. 1993; 93(3): 337-343.

Malumbres M, Barbacid M. Mammalian cyclin-dependent kinases. Trends Biochem Sci. 2005; 30(11): 630-641.

Marshall NF, Peng J, Xie Z, Price DH. Control of RNA polymerase II elongation potential by a novel carboxyl-terminal domain kinase. J Biol Chem. 1996; 271(43): 27176-27183.

McCune JM. The dynamics of $CD4^+$ T-cell depletion in HIV disease. Nature. 2001; 410(6831): 974-979.

Mitsuyasu RT. Non--AIDS-defining malignancies in HIV. Top HIV Med. 2008; 16(4): 117-121.

Nechaev S, Adelman K. Pol II waiting in the starting gates: Regulating the transition from transcription initiation into productive elongation. Biochim Biophys Acta. 2011; 1809(1): 34-45.

Ou M, Sandri-Goldin RM. Inhibition of cdk9 during herpes simplex virus 1 infection impedes viral transcription. PLoS One. 2013; 8(10): e79007.

Palermo RD, Webb HM, West MJ. RNA polymerase II stalling promotes nucleosome occlusion and pTEFb recruitment to drive immortalization by Epstein-Barr virus. PLoS Pathog. 2011; 7(10): e1002334.

Peyressatre M, Prével C, Pellerano M, Morris MC. Targeting cyclin-dependent kinases in human cancers: from small molecules to Peptide inhibitors. Cancers (Basel). 2015; 7(1): 179-237.

Price DH. P-TEFb, a cyclin-dependent kinase controlling elongation by RNA polymerase II. Mol Cell Biol. 2000; 20(8): 2629-2634.

Prichard MN, Daily SL, Jefferson GM, Perry AL, Kern ER. A rapid DNA hybridization assay for the evaluation of antiviral compounds against Epstein-Barr virus. J Virol Methods. 2007; 144(1-2): 86-90.

Prichard MN, Hartline CB, Harden EA, Daily SL, Beadle JR, Valiaeva N, Kern ER, Hostetler KY. Inhibition of herpesvirus replication by hexadecyloxypropyl esters of purine- and pyrimidine-based phosphonomethoxyethyl nucleoside phosphonates. Antimicrob Agents Chemother. 2008; 52(12): 4326-4330.

Rechter S, Scott GM, Eickhoff J, Zielke K, Auerochs S, Müller R, Stamminger T, Rawlinson WD, Marschall M. Cyclin-dependent Kinases Phosphorylate the Cytomegalovirus RNA Export Protein pUL69 and Modulate Its Nuclear Localization and Activity. J Biol Chem. 2009; 284(13): 8605-8613.

Romano G, Giordano A. Role of the cyclin-dependent kinase 9-related pathway in mammalian gene expression and human diseases. Cell Cycle. 2008; 7(23): 3664-3668.

Santo L, Vallet S, Hideshima T, Cirstea D, Ikeda H, Pozzi S, Patel K, Okawa Y, Gorgun G, Perrone G, Calabrese E, Yule M, Squires M, Ladetto M, Boccadoro M, Richardson PG, Munshi NC, Anderson KC, Raje N. AT7519, A novel small molecule multi-cyclin-dependent kinase inhibitor, induces apoptosis in multiple myeloma via GSK-3beta activation and RNA polymerase II inhibition. Oncogene. 2010; 29(16): 2325-2336.

Schang LM. Cyclin-dependent kinases as cellular targets for antiviral drugs. J Antimicrob Chemother. 2002; 50(6): 779-792.

Scrace SF, Kierstan P, Borgognoni J, Wang LZ, Denny S, Wayne J, Bentley C, Cansfield AD, Jackson PS, Lockie AM, Curtin NJ, Newell DR, Williamson DS, Moore JD. Transient treatment with CDK inhibitors eliminates proliferative potential even when their abilities to evoke apoptosis and DNA damage are blocked. Cell Cycle. 2008; 7(24): 3898-3907.

Silvestri G, Fedanov A, Germon S, Kozyr N, Kaiser WJ, Garber DA, McClure H, Feinberg MB, Staprans SI. Divergent host responses during primary simian immunodeficiency virus SIVsm infection of natural sooty mangabey and nonnatural rhesus macaque hosts. J Virol. 2005; 79(7): 4043-4054.

Tamrakar S, Kapasi AJ, Spector DH. Human cytomegalovirus infection induces specific hyperphosphorylation of the carboxyl-terminal domain of the large subunit of RNA polymerase II that is associated with changes in the abundance, activity, and localization of cdk9 and cdk7. J Virol. 2005; 79(24): 15477-15493.

Wang S, Fischer PM. Cyclin-dependent kinase 9: a key transcriptional regulator and potential drug target in oncology, virology and cardiology. Trends Pharmacol Sci. 2008; 29(6): 302-313.

Yamada T, Yamaguchi Y, Inukai N, Okamoto S, Mura T, Handa H. P-TEFb-mediated phosphorylation of hSpt5 C-terminal repeats is critical for processive transcription elongation. Mol Cell. 2006; 21(2): 227-237.

Yu DS, Cortez D. A role for CDK9-cyclin K in maintaining genome integrity. Cell Cycle. 2011; 10(1): 28-32.

Zhang H, Park SH, Pantazides BG, Karpiuk O, Warren MD, Hardy CW, Duong DM, Park SJ, Kim HS, Vassilopoulos A, Seyfried NT, Johnsen SA, Gius D, Yu DS. SIRT2 directs the replication stress response through CDK9 deacetylation. Proc Natl Acad Sci U S A. 2013; 110(33): 13546-13551.

Zhang J, Li G, Ye X. Cyclin T1/CDK9 interacts with influenza A virus polymerase and facilitates its association with cellular RNA polymerase II. J Virol. 2010; 84(24): 12619-12627.

Zhou Q, Yik JH. The Yin and Yang of P-TEFb regulation: implications for human immunodeficiency virus gene expression and global control of cell growth and differentiation. Microbiol Mol Biol Rev. 2006; 70(3): 646-659.

7. ACKNOWLEDGMENTS

I would like to thank my supervisor Professor Marco Pittau.

I would like to express my gratitude to Dr Franco Lori and Sjlva Petrocchi for giving me the opportunity to do my PhD while continuing my work at ViroStatics.

I would also like to acknowledge James Chafouleas, Marco Adami and Ennio Cavalletti for the great discussions during the drug development process.

Thanks to my collegues at ViroStatics Barbara Poddesu, Giulia Cugia, Simona Caleffi for supporting in the daily lab work.

Lastly, I would like to say a big thanks to my wonderful family, my wife Michela and my kids, Gabriele, Giulio and Elisa.